



THE UNIVERSITY of EDINBURGH School of Geosciences

David Lundbek Egholm
Associate Editor, Earth Surface Dynamics

Guillaume C.H. Goodwin
School of Geosciences
University of Edinburgh
Drummond Street
Edinburgh, EH8 9XP
Phone: +44 (0)131 650 2537
Email: g.c.h.goodwin@sms.ed.ac.uk

January 31, 2018

Dear Prof. Egholm,

Thank you for considering our manuscript ‘Unsupervised detection of salt marsh platforms: a topographic method’. We are grateful to the reviewers for providing constructive feedback which has helped us to improve the manuscript.

The reviewers were primarily concerned with providing more evidence that the Topographic Identification of Platforms (TIP) method is applicable to a wide range of salt marsh platforms. They justly noted that the method was tested exclusively on sites within the United Kingdom which, although representative of many salt marsh environments, do not encompass (1) American salt marshes, (2) microtidal environments and (3) prograding salt marshes. We addressed these concerns by testing the TIP method on three additional sites in the United States: Morro Bay, CA, Wax Lake Delta, LA and Plum Island, MA. The performances of the TIP method on these sites are reported in Appendix B of the revised manuscript.

Another important comment made by both reviewers was that our original manuscript did not highlight the limitations of the TIP method clearly enough in relation to the design of the method. In order to respond to these comments we modified the structure of our manuscript, including an additional section dedicated to the influence of site properties on results of the TIP method. Appendix B also contains analysis of additional site morphologies that push the limits of the TIP method, as well as providing guidance on the applicability of our method when analysing salt marshes in challenging environments.

Please find below detailed responses to the individual points raised by each of the reviewers, along with a version of our manuscript highlighting the changes we have made to answer the reviewer comments. We have formatted *reviewer comments in italics*, and our responses are in normal font. Throughout our responses we refer to line numbers in our manuscript: these are the correct line numbers in the manuscript with the changes incorporated. We have endeavoured to address all concerns and return the manuscript in a publication-ready state.

Sincerely,
Guillaume Goodwin
Guillaume C.H. Goodwin

Reviewer 1

We thank the reviewer for their helpful suggestions. Below we describe how we adjusted the manuscript in the revised version in response to these comments.

Comment 1: *I worry that the authors may underestimate the level of detail needed to accurately resolve the decimeter scale topography of the marsh platform in the requisite DEM. The authors rely heavily on widely available Lidar DEMS for the TIP method despite the fact that the overall relief of the marsh platform is often missed completely by Lidar sensors. Perhaps it doesn't really matter here since the authors are establishing marsh platform identification on the scarp perimeters...but, I wonder if there are any ways you might improve on your method to extend its usefulness to other marsh landscapes (those without scarps, and those characteristic of patchy, discontinuous areas of marsh platform that might be heavily dissected by intertidal creek networks).*

The reviewer is entirely correct to point out that some scarp heights may be lower than the vertical accuracy of the lidar data. This resolution and the relief plays a role in selection of the minimum scarp height: please see our response to reviewer 2. We included more sites in the appendix that push the limits of the method (e.g. in very low relief landscapes). We have used the method on the Wax Lake Delta in Louisiana, and the method can detect the marsh where scarps are apparent despite the fact that the maximum relief of the point cloud is 80 cm (including the returns from vegetation).

We do want to point out that our test sites have used widely available lidar DEMs: in our test cases the method works well, and the scarps/platforms are correctly delineated by the algorithm. As suggested by the reviewer, the precise topography of the platform is not necessary for the TIP method to function, as our method is focused on detecting scarps and filling the platforms at areas of higher elevation, rather than relying on the elevations of the platform itself. This has the effect of making the TIP method less sensitive to unequal removal of vegetation between different DEM sources. In response to comments below we included a few more sites with smaller tidal ranges in the appendix, and added more cautionary language about the use of the method. However, we would also like to make clear that the method can work on microtidal marshes as long as there are scarps (more on that point later). Three examples of American salt marshes were added in Appendix B of the revised manuscript.

We chose not to include patch detection or tidal creek detection in the TIP method for this manuscript. This requires the implementation of different algorithms as they have distinct morphological characteristics, and we feel this is a different topic. We agree with the reviewer that such an algorithm would be very beneficial, but we feel this is beyond the scope of the current manuscript. We have, however, tested the TIP method on expanding patches (see the results for Wax Lake Delta in Appendix B of the revised manuscript).

Comment 2: *The method presented here is only useful in marsh landscapes characteristic of steep scarps (as in erosional environments). I think that the title should reflect that in some way.*

The term 'platform' in the title is meant to reflect the necessity of the presence of a scarp in our method. We added the following definition: 'We here define salt marsh platforms as sub-horizontal surfaces in the coastal landscape, separated from surrounding intertidal flats by steep scarp features.' on P3L9 to clarify this point.

We do feel this comment suggests the method is somehow a niche method only applicable to limited settings. The authors have personally conducted field campaigns across marshes in northern France (in a macrotidal environment), in northern Italy (in microtidal environments), across the UK (along a range of sea level rise rates and tidal ranges), along the Atlantic coast of the United States

(South Carolina and North Carolina) and in the Gulf Coast of Florida. We have also recreationally visited marshes in Louisiana, California and Oregon. In all cases these marshes had platforms and scarps, despite the wide variety in vegetation species, tidal range, sea level rise rates, suspended sediment concentrations, temperatures, and wave climates. We acknowledge not all marshes have scarps and therefore not all marshes are amenable to the TIP approach, but we do wish to emphasise that this method should be broadly applicable over a wide range of geographic areas. In Appendix B we added three sites outside of the UK to demonstrate the method is not limited to the 6 specific sites we chose for intensive method verification. These places were also chosen to highlight places where the algorithm is unlikely to work to ensure that readers are aware of any pitfalls.

Comment 3: *Perhaps you could include more descriptive information on the geomorphology of your study sites. For instance, you have high resolution DEMs for all, why not calculate drainage density, or some other metric to describe how heavily dissected the marsh platform is? Then, your results could vary as a function of drainage density and tidal range? Maybe. . .*

We agree with the reviewer that it could be useful to look at the performance of the method in platforms with different degrees of dissection. Having published previously on drainage density (Clubb et al., 2016, JGR-ES, doi:10.1002/2015JF003747), we are slightly wary of using this specific metric. Drainage density is defined as the length of the channels in a basin divided by the basin area, but basin area in a marsh context is extremely difficult to quantify. Furthermore, many tidal channels in marsh environments are wide compared to the size of marsh features.

In the revised manuscript, we added the following text in section 4.2: ‘As a proxy for the dissection of the platform by tidal creeks, we digitise tidal creek centrelines from the DEM. We then calculate the total length of tidal creeks included in the digitised platform divided by the platform surface area. We refer to this quantity as the Dissection Index (DI). In Fig. 11, we examine the capacity of the TIP-method to determine the area and perimeter of marsh platforms according to their dissection index. We find that for all test sites, TIP-detected area remains within 10% of the digitised area, whereas TIP-detected perimeter increases steadily with Dissection Index, confirming that the exclusion of tidal creeks by the TIP method is consistently stricter than by digitisation.’

Figure 11 was modified to have Dissection Index on the x-axis, thus highlighting the influence of dissection on the relative performances of the TIP method and digitisation.

Comment 4: *The paper could use some organizational finesse to improve the flow of the narrative. There are many instances where results are stated in the Methods section, and there is no Discussion section, but discussion elements are mixed in with Results. I would also consider adding a separate section for Validation following or within the Methods section to describe how you evaluated the performance of the TIP method. It seems very out of place in its current position (Results and Discussion). See specific comments below*

In order to make our manuscript clearer, we modified the structure to the following:

1. Introduction
2. Methodology
 - (a) Test sites
 - (b) Preprocessing Topographic Data
 - (c) Scarp routing
 - (d) Platform identification

3. Results

- (a) Parameter optimisation
- (b) Validation and applicability

4. Discussion

- (a) Influence of site morphology the TIP method
- (b) Future developments
- (c) Potential for monitoring

5. Conclusions

Comment 5: *The Results section is a bit messy. Perhaps consider organizing into a more logical manner. For instance, I like the idea of presenting results as a function of tidal range (or drainage density see comment 3). . .start with S1, describe, then go on to S2. . .and so on. Then, in a separate section (see comment 4) you could demonstrate the effects of using the filter on TIP results. I think this approach would be fine, because you already told us that you dont want to use the filter. . .and thats OK.*

As mentioned in our response to comment 4, we reorganised our manuscript to improve its clarity and better follow the order of the figures. We have followed some of the reviewers suggestions, for example more granularity in the results section as well as separating results and discussion. However, we did not order the results on a site-by-site basis as we believe it would lead to a much longer results section, as well as making it more difficult to link results from different sites when illustrating our discussion and demonstrating the overall performance of the TIP method.

P1L3: The productivity and even survival of salt marsh. . .(remove even).

This modification was made.

P1L3: . . .of salt marsh vegetation. . .(why vegetation here? Why not landscape? Seems out of place.)
This was changed to ‘the sustained existence of the salt marsh ecosystem’

P1L5, P1L7, P1L15

The suggested changes were made

P1L20: . . ., it also suggests. . . (what is it?)

This was changed to ‘we suggest’

P2L9: awkward, consider revising. . .perhaps something like, . . .makes monitoring the evolution of salt marshes imperative for management strategies and scientific endeavors. . .

The original text was replaced by: ”makes monitoring the evolution of salt marshes crucial for developing management strategies that maintain the health of these ecosystems.”

P2L34: Right. . .but marsh platform slopes are on the order of 30cm total relief. . .and the overall structure is often misrepresented by lidar sensors with a nominal accuracy of +/- 15cm.

The vertical accuracy (z-accuracy) of airborne lidar and photogrammetry may indeed be close to the size of the smallest scarps, which may be 30 cm or less in height for micro-tidal areas, immature platforms or marshes situated high in the tidal frame. If we consider an unvegetated surface (or a ‘cleaned’ DSM), we argue that the nominal accuracy is a combined product of georeferencing and distance-measurement accuracy of the lidar itself, the georeferencing generally accounting for the main part of the vertical error. The TIP method is focused on relative elevations in local neighbourhoods, and is therefore not very sensitive to the z-accuracy. If we consider a vegetated surface however, DEM processing (such as ground-return filtering and rasterisation) may indeed lead to higher and more locally disparate z-accuracy values on the platform than on the tidal flat. We argue in section 4.1 that the presence of vegetation induces positive errors, which plays in favour of the TIP method, as this artificially increases the platform height and therefore the scarp slope. To highlight these points, we have included an

example of very low relief marsh, Wax Lake Delta, and a marsh with low local relief, Morro Bay marsh, for which the TIP method successfully identifies the marsh platform.

P3L19: . . .horizontal resolutions. . .(do you mean horizontal extents? These are two very different things.)

By horizontal resolution we mean the grid cell size of a rasterised DEM. The text was amended to read 'at varying grid cell sizes' to signify that all six sites were examined at different grid cell sizes.

P3L20: remove dash after short.

We made this change.

P3L29: can you provide any technical specs for the lidar survey? Seasonality? Tides? Etc. . .

We included a link to the metadata for Environment Agency lidar. The exact flight times relative to tides are unknown, however lidar surveys by the EA are conducted around low tide.

P4L6: stronger than what?

We now say: 'subject to a spring tidal range of 3.8 m and fluvio-tidal currents due to their estuarine fringing position'. *P4L9: . . .provides. . .(change to provide)*

We made this change.

P4L10: what do you mean by numerous? How many more channels are at this site compared to the others? Consider using more physical descriptors throughout your study site description. What are the respective areas?

Figure 11 of the revised manuscript provides a measure of the dissection of each marsh platform.

P4L12: What do you mean by levels? Elevation? Water level?

We replaced this with 'elevations'.

P4L21: Why three times the horizontal resolution of the DEM? Why not 5 or 6?

We now say: 'selected because it is the minimum radius needed to calculate slope with this method'.

P4L31-33: At what scale is this problematic? 100s of kilometers? 10s of kilometers? I thought we were focused on relatively small areas of marsh landscape. . .what are the relative sizes of each study site (see also comment P4L10 above).

The sites considered here are indeed small section of marshes. However, the local definition of kernels is unaffected by the DEM extent. The calculation time would however increase for larger marshes. At the time of writing, we have not tested the method on marshes larger than 12 km², for which the method did not encounter difficulties, despite the longer run times. Dimensions of the sites are included in the caption of Figure 10 of the revised manuscript. We replaced the original formulation by 'Likewise, although marsh platforms are locally higher than tidal flats and channels, this may not be the case for complex depositional environments (e.g. marshes sheltered by a sand spit), where long-shore declivity may cause portions of the tidal flats to be higher than distant emergent platforms' to better make our point.

P5L9-22: Can you briefly describe what each of these means physically and the importance of information provided by each?

Although the non-dimensional values of elevation and slope indeed have physical meaning, we did not wish to detail extensively as this would require investigation into formative processes for each site and considerably lengthen the manuscript. The aim of the manuscript is not to explore the history of the six test sites but rather to demonstrate the general applicability of the method, and these metrics are solely a means for us to apply the method over different landscapes.

P5L24 (and throughout): be careful to avoid stating results in Methods section.

We have now separated these as requested by the reviewer.

P5L25: what is pdf? define.

'pdf' is here defined as a probability distribution function: this is now clear in the text.

P6L20: large number of true scarps? Or do you mean large number of misidentified scarps that are actually creek banks?

This procedure produces a large number of scarps that could be creek banks and local DEM irregularities.

We now say 'This procedure produces a large number of potentially misidentified scarps, as small creeks within the platform and in higher portions of the tidal flat tend to be selected during this procedure.'

P7L7: why 11?

11 is a value we chose to obtain a significantly wider kernel. Other values have not been tested.

P7L16 (and throughout), P7L27 (and throughout), P8L2

We made these changes.

P8L11 (throughout): Methods presented in results section. Consider providing a separate subsection in Methods for validation and then share results in the proper Results section.

We did this: see response to Specific Comment 4.

P8L12-15: Im guessing TP, FN, etc. . . are obtained from subtracting? Maybe show that in Methods. TP are obtained by counting the number of boolean True values for the detected marsh and the digitised marsh. Same for FP, etc. We now include the specifics in section 2.5 on performance metrics.

P9L1: . . .the manual digitization. . .did you even discuss that in your Methods section? What software was used? Scale?

The details were already provided in the Methods section.

P9L14 - line number no longer applies in the revised manuscript: describe one figure at a time, and in chronological order.

See response to Specific Comment 4.

P9L19-29 - line number no longer applies in the revised manuscript: discussion in Results section. Consider revising.

See response to Specific Comment 4.

P10L23: Isnt this simply a transition zone between marsh platform and tidal flat?

Although these zones correspond topographically to transition zones, they might not be vegetated (which was observed on aerial imagery for this site), and potentially unstable. We have therefore not called them 'pioneer zones' to avoid confusion with vegetated transition zones.

P10L26: . . .saltings. . .why are you defining this here? You referred to salting earlier with no definition. Define earlier.

Saltlings were replaced by 'fallen blocks' to avoid confusion.

P10L17: . . .yes, but its limited to erosional landscapes with obvious scarps.

See response to comment 1. The reviewer quite correctly notes that this is limited to marsh landscapes with erosional scarps. This fits with our definition of 'salt marsh platform'. However this morphology is extremely common in salt marshes across a wide range of environments: many Atlantic and Gulf coast marshes in North America, many UK marshes (and all we have examined for this paper), marshes along the north coast of France, marshes in Italy, and these are just the examples that the authors have personally visited. So we believe the method is applicable to a significant fraction of global salt marshes.

P11L9: . . .algae. . .why is this here?? Did you test for this or are you speculating? Maybe you could instead say that your method works independent of such environmental factors. . .its implied, but not exactly tested for in this paper.

We see that this was inelegantly introduced into the paper. It is here for a reason, however: initially when we started identifying marshes it was suggested to us that we simply use optical techniques. However in our imagery, and in particular at Shell Bay, algae and biofilms are widespread making much of the landscape green. We wanted to make the point that even if the landscape is green from algae, or if there are widespread biofilms, we could still detect a marsh platform. Of course, large accumulations of macro-algae (kelp, etc.) might trick the method. We now clarify this by saying 'Furthermore, the presence of algae, kelp or duckweed as well as varying vegetation reflectance properties, which may induce specific calibrations with spectral methods (Morris et al., 2005), do not affect our results (barring mounds of stranded algae large enough to affect topography).'

Figure 3, 5, 7, 9, 11

The suggested changes were made.

Figure 8: maybe a table would be a nice complement to this figure?

A table for each subplot was added in Appendix A.

Figure 10: scale?

Scale is included in text to avoid clutter on these already crowded maps.

Reviewer 2 We would like to thank the reviewer for their comments and positive response to our manuscript. In our revised manuscript we will make the following changes in light of the reviewer's helpful suggestions.

My only concern is that the methodology is presented as a general tool for salt marsh and tidal flat identification, while I believe that its application is limited to the specific type of marshes presented in this study. I suggest the authors to:

Suggestion 1: better clarify the specs of the methodology that are tightly linked to the morphological characteristics of the specific study sites in order to make aware the user of the limits in applying the methodology

We took the point of this comment, similar to comments made by Reviewer 1, and added text on the limitations of the method (especially in low relief or emergent marshes). We also added some more example marshes in Appendix B to demonstrate the method's results beyond the UK. See responses to reviewer 1 for specific text additions.

Again, we do feel it necessary to clarify that the TIP method is not site specific. It has been designed to apply to a wide variety of marshes and not only the test sites. We tested the method across a number of sites in the United Kingdom because these sites have a wide range of tidal range and wave climates. The basic features the method extracts, namely flat areas separated by scarps, are common to many marsh environments (albeit with some exceptions, which we will describe in the revised text). We acknowledge that the UK sites do not have a large variety of vegetation types, but in general the basic geometry of marshes is common across salt marshes, from the macrotidal Mont Saint Michel estuary to the microtidal Venice lagoon, which have rather different vegetation assemblages. Marshes along the Gulf and Atlantic coasts of North America also share the common morphology of flat areas separated by scarps. The stabilisation of deposited sediment and increased deposition rates (by direct trapping and velocity reduction) induced by vegetation are processes that occur in salt marshes regardless of their geographical location and local forcings. This process leads to the bifurcation of salt marsh platforms from tidal flats, leading to the formation of scarps (Mariotti and Fagherazzi 2010, DOI: 10.1029/2009JF001326). The TIP method therefore hinges only on the existence of a scarp and its representation on a DEM. The method does not depend on other morphological features save the absence of a very large river channel in the tidal flat.

In the revision we have explored marshes that are likely to be at the limits of the TIP method's ability to detect marshes and summarised for the reader the conditions that limit the method's accuracy, as suggested by the reviewer. We tested our method on the Wax Lake Delta, LA, a marsh with very low relief, and the Plum Island marsh, MA, a site heavily influenced by human activity, as well as Morro Bay, CA, where relief is locally very low. We find that the method can detect the marsh platform successfully in all three environments, but is challenged by the presence of prograding patches of vegetation.

Suggestion 2: describe in more details the 6 study sites considered in this research underlying the specific peculiar morphological characteristics. This will allow the user/reader to decide if the

methodology may be applied to a different study site. Moreover, the authors refer to a 20 cm value to be subtracted to define the minimum local elevation for a platform pixel (pag. 7 lines 7-8). Also in this case a more precise explanation should be included so that the reader can judge if this is a value typical of the considered study sites or can be generalized.

We have added more text on limitation of the method in the method and discussion sections, and have added an appendix with more sites with different vegetation assemblages and tidal regimes. For the 20 cm threshold we now say in the method section: 'The algorithm will not identify as separate platforms separated by scarps less than this elevation threshold, so on microtidal marshes this threshold can be lowered. We address this limitation in the discussion and appendix. The threshold is necessary to prevent the algorithm from excluding pools and slight depressions in the platform surface.'

As mentioned in the methods section, the discussion (section 4.2) now reads: 'The morphological characteristics of prograding marshes are different from those of established platforms: consequently, vegetation patches and pioneer zones are not the object of the TIP method. Specifically, prograding margins and vegetation patches tend to have a relief and slope that are close to those of the tidal flat, making their outlines invisible to the scarp routing process. The combined absence of scarps and low relief of prograding marshes then interfere with the 20 cm leeway included in the platform filling process and cause an excess of false positives. Users may reduce this leeway to improve accuracy (see Fig.B2b1), but we discourage the use of the TIP method to identify vegetation patches and prograding margins.'

Pag. 5 lines 20-25: in the text I do not see a description of the gray area in Fig. 3a.

The grey area in Fig3a corresponds to the values of P^* to be excluded from the initial search space. This was already present in the caption.

Pag 7 lines 7-10: Is the value 20cm applied to all the study sites? Could you please better explain how this specific value has been selected? is there a relation with the tidal excursion for example? Is this value specific for the English study sites?

See comments above in response to suggestion 2. To summarise: the 20cm threshold works in all but one of our test cases including the microtidal site at Morro Bay. It fails at Wax Lake Delta where the total elevation range, including vegetation, is 80 cm. So the 20 cm threshold works in all but the most low relief sites. We have added text to this effect in the revision (specifics can be found in response to suggestion 2).

Figure 12: the faded lines are difficult to see

In the revision we slightly modified the colours of the lines. Faded lines are however covered by bright lines in most cases, and this was clarified in the caption.

Unsupervised detection of salt marsh platforms: a topographic method

Guillaume C. H. Goodwin¹, Simon M. Mudd¹, and Fiona J. Clubb^{1,2}

¹School of Geosciences, University of Edinburgh

²Institute of Earth and Environmental Science, University of Potsdam, Germany

Correspondence to: Guillaume C. H. Goodwin (g.c.h.goodwin@sms.ed.ac.uk)

Abstract.

Salt marshes filter pollutants, protect coastlines against storm surges, and sequester carbon, yet are under threat from sea level rise and anthropogenic modification. The ~~productivity and even survival of salt marsh vegetation sustained existence of the salt marsh ecosystem~~ depends on the topographic evolution of marsh platforms. Quantifying marsh platform topography is vital for improving the management of these valuable landscapes. ~~Determining~~ The determination of platform boundaries currently relies on supervised classification methods requiring near-infrared data to detect vegetation, or demands ~~labor-intensive~~ labour-intensive field surveys and ~~digitization~~ digitisation. We propose a novel, unsupervised method to reproducibly isolate ~~saltmarsh~~ salt marsh scarps and platforms from a DEM, referred to as Topographic Identification of Platforms (TIP). Field observations and numerical models show that ~~saltmarshes~~ salt marshes mature into sub-horizontal platforms delineated by sub-10 vertical scarps. ~~based~~ Based on this premise, we identify scarps as lines of local maxima on a slope raster, then fill landmasses from the scarps upward, thus isolating mature marsh platforms. We test the TIP method using lidar-derived DEMs from six ~~saltmarshes~~ salt marshes in England with varying tidal ranges and geometries, for which topographic platforms were manually ~~distinguished~~ isolated from tidal flats. Agreement between manual and unsupervised classification exceeds 94% for DEM resolutions of 1 m, with all but one ~~sites~~ site maintaining an accuracy superior to 90% for resolutions up to 3 m. For resolutions of 15 1 m, platforms detected with the TIP method are comparable in surface area to ~~digitized~~ digitised platforms, and have similar elevation distributions. We also find that our method allows for the accurate detection of local ~~blee~~ block failures as small as 3 times the DEM resolution. Detailed inspection reveals that although tidal creeks were ~~digitized~~ digitised as part of the marsh platform, unsupervised classification categorizes them as part of the tidal flat, causing an increase in false negatives and overall 20 platform perimeter. This suggests our method ~~would have increased accuracy if used in~~ may benefit from combination with existing creek detection algorithms. Fallen ~~bloes~~ blocks and high tidal flat portions, associated with potential pioneer zones, ~~may also be areas of diseordanee~~ can also lead to differences between our method and supervised mapping. Although pioneer zones prove difficult to classify using a topographic method, ~~it also suggests~~ we suggest that these transition areas should be considered when analysing erosion and accretion processes, particularly in the case of incipient marsh platforms. Ultimately, we have shown that unsupervised classification of marsh platforms from high-resolution topography is possible and sufficient 25 to monitor and ~~analyze~~ analyse topographic evolution.

1 Introduction

Salt marshes are highly dynamic ecosystems, ~~sequestrating~~ sequestering on average $210 \text{ g CO}_2 \text{ m}^{-2} \text{ yr}^{-1}$ through plant growth and decay (Chmura et al., 2003) and capturing additional inorganic sediment when they are submerged (Nardin and Edmonds, 2014). This productivity has allowed salt marshes to match historic sea level rise (Kirwan and Temmerman, 2009) and laterally 5 expand when sediment inputs were sufficient (Kirwan et al., 2011). It also places them among the most valuable ecosystems in the world (Costanza et al., 1997), and they provide diverse ecosystem services such as flood attenuation (Möller and Spencer, 2002; Shepard et al., 2011), blue carbon sequestration (Chmura et al., 2003; Coverdale et al., 2014), and contaminant capture (Nelson and Zavaleta, 2012). Their economic value combined with their alarming retreat (Day et al., 2000; Duarte et al., 2008; Kirwan and Megonigal, 2013) makes monitoring the evolution of salt marshes ~~a pressing management imperative as well as a~~ 10 ~~scientific endeavor~~ crucial for developing management strategies that maintain the health of these ecosystems.

The most closely monitored properties of salt marsh ecosystems are ecological assemblages and elevation, as they are both essential to understand ~~eeogeomorphic~~ eco-geomorphic processes (Reed and Cahoon, 1992). For instance, elevation determines flooding frequency and therefore influences pioneer vegetation encroachment (Hu et al., 2015), which in turn affects vertical 15 accretion through inorganic sediment capture (Pennings et al., 2005; Mudd et al., 2004, 2010). Individual plants also react to elevation by modifying their root to shoot length ratios, generating feedbacks between organic material build-up and sediment capture (Mudd et al., 2009). The variable intensity of these ~~eeogeomorphic~~ eco-geomorphic feedbacks enables salt marshes to accrete in response to variations in sea level, thus maintaining their place in the tidal frame (Kirwan and Temmerman, 2009; Crosby et al., 2016).

The objective detection and analysis of vegetation patterns is a mature field, with habitat mapping commonly undertaken 20 through the analysis of spectral properties such as the Normalized Difference of Vegetation Index (NDVI) (Jucke van Beijma, 2015). NDVI mapping is now ~~mature~~ developed to the extent that it requires only a minimum of ground-truthing to determine the presence and type of vegetation (Hladik and Alber, 2014). This index has been shown to consistently differentiate vegetated areas from tidal flats (Tuxen et al., 2008) and flooded channels from dry land despite the sensitivity of classification algorithms (Belluco et al., 2006; Wang et al., 2007).

25 ~~Spectral data sources, however, are not sufficient to~~ However, spectral data sources do not provide the topographic information necessary to fully understand morphodynamic processes: although Digital Elevation Models (DEMs) have been successfully generated from habitat maps in the Venice lagoon (Silvestri et al., 2003), additional influences on halophyte distribution such as groundwater circulation (Moffett et al., 2010, 2012) can lead to mismatches between topography and habitats (Hladik et al., 2013). These additional influences on habitat distribution prevent the reliable use of spectral data to infer topography. Furthermore, delineating salt marsh platforms exclusively from spectral sources encourages morphological studies to 30 define salt marshes dominantly from an ecological perspective, whereas the physical setting, most notably the elevation within the tidal frame, plays a key role in maintaining ecosystem health (e.g., Morris et al., 2002).

The topographic data necessary to identify marsh platforms already exist: the ~~multiplication~~ proliferation of freely available high resolution topographic datasets from lidar or structure from motion (SfM) techniques means that DEMs ~~of horizontal~~

~~resolutions~~ with a grid cell size below 1 m are increasingly common on salt marshes, and offer vertical accuracies below 20 cm even without correcting for vegetation (Sadro et al., 2007; Wang et al., 2009; Chassereau et al., 2011). At these resolutions, most scarps and channels are detectable on a DEM, and several automated topographic methods already allow the identification of tidal channel networks (Fagherazzi et al., 1999; Liu et al., 2015). However, contrary to spectral datasets, tools designed to 5 accurately delineate the extent of salt marshes through means other than manual ~~digitization~~ ~~digitisation~~ are lacking.

In this study, we propose an unsupervised method to topographically differentiate marsh platforms from tidal flats, which we refer to as Topographic Identification of Platforms (TIP). The TIP method aims to reproducibly and accurately delineate marsh platforms using only a DEM as input, while also reducing identification costs and enabling systematic topographic analyses of multiple salt marshes.

10 We here define salt marsh platforms as sub-horizontal surfaces in the coastal landscape, separated from surrounding intertidal flats by steep scarp features. The processes that form salt marsh platforms can be described by ecological alternate stable states theory (Schroder et al., 2005) and geomorphic bifurcation models (Fagherazzi et al., 2006; Defina et al., 2007). These processes cause salt marshes to develop a distinctive, biologically-mediated topographic structure consisting of several sub- 15 horizontal platforms, separated from tidal flats and from each other by a subvertical scarp and dissected by incising channels (Temmerman et al., 2007; Marani et al., 2007, 2013). The TIP method exploits this characteristic topography, which is clearly visible on high-resolution DEMs and their associated slope rasters, to identify scarps and steep channel banks. As our method uses topographic signatures of marsh platforms, it will reflect the interplay between sedimentation, erosion, and biomass (Fagherazzi et al., 2012) rather than the distribution of specific macrophyte species ~~and~~. It should therefore be complementary to, rather than a replacement for, methods that detect plant zonation on marshes. We compare TIP-detected platforms with 20 six manually ~~digitized~~ ~~digitised~~ platforms from English marshes ~~of different horizontal resolutions at varying grid cell sizes~~, demonstrating the potential of this method for quantitative topographic analyses and ~~short~~ ~~short~~ to mid-term monitoring.

2 Methodology

The TIP method automatically detects scarps and platforms of salt marsh systems from a DEM with no manual calibration requirements. Its general process is described in Fig. 1, and includes the possibility of filtering (step 1) and degrading (step 2) 25 the DEM; the effects of both treatments are examined in the discussion. A slope raster is then generated by fitting a polynomial surface to topographic data and taking the derivative of this surface (Hurst et al., 2012; Grieve et al., 2016) (step 3). Steps 4 and 5 are novel algorithms developed in this study to isolate scarps and platforms. The results of the isolation process are compared to manually generated platforms (step 6) to generate a comparison map (step 7).

2.1 Test sites

30 We test the TIP method on six sites in England, selected for the availability of airborne lidar data in the form of gridded 1 m resolution rasters, provided by the UK Environment Agency (<http://environment.data.gov.uk/ds/survey/>), and for the diversity of their morphologies and tidal ranges. Dataset metadata is available freely on the Environment agency website

(<https://data.gov.uk/dataset/lidar-composite-dtm-1m1>). For each site, marsh platforms were ~~digitized~~ digitised on an unfiltered and non-degraded DEM at a scale of 1: 2,500, using the open-source software QGIS (step 6 in Fig. 1). Source data were flown in 2012 for all sites, unless noted otherwise. The locations of the selected sites are shown in Fig. 2.

Shell Bay, Dorset (S1) is a shallow bay with a spring tidal range of 2.4 m, located in Poole Harbour, a limited entrance bay (sensu Allen (2000)) protected from strong waves. The marshes in Shell Bay display jagged outlines, indicative of low wave and tidal current stress (Leonardi and Fagherazzi, 2014). The Stour Estuary marshes (S2) 6 km upstream of the meso-tidal Stour mouth are subject to a spring tidal range of 3.8 m and ~~stronger tidal~~ fluvio-tidal currents due to their estuarine fringing position (sensu Allen (2000)), and therefore display more linear boundaries. The Stiffkey marshes (S3) are back-barrier marshes (Allen, 2000), which experience a 4.7 m spring tidal range and display signs of erosion and accretion. These recent perturbations to the marsh surface ~~provides~~ provide an interesting challenge for topographic detection of marsh extents. The macro-tidal Medway estuary marshes (S4, spring tidal range of 6.4 m) were chosen due to the presence of numerous channels in the tidal flats. In order to test the ability of our method in regions with extreme tidal ranges, we also analysed two mega-tidal sites: Jenny Brown's Point marshes (S5, spring tidal range of 9.2 m) and the Parrett estuary (S6, spring tidal range of 11.8 m), where sand dunes, different ~~levels~~ elevations inside the tidal flats, ~~saltings~~ fallen blocks and sunken platforms will test the limits of the method's ability to correctly delineate marshes in these environments.

2.2 Preprocessing Topographic Data

The TIP method isolates marsh platforms from a DEM up to their seaward limits by detecting the topographic signature generated by the development of salt marshes. The definition of landward boundaries can vary significantly with context, and may be defined by a vegetation zonation change (Mo et al., 2015), agricultural parcels, or infrastructure (Feagin et al., 2010). Topographic input data is therefore clipped to the landward limit of the platform, at the discretion of the user. In the preparation stage, local slope is calculated from the DEM by fitting a second order polynomial surface (Hurst et al., 2012) with a ~~ei~~ regular ~~window radius equal to~~ window radius of three times the horizontal resolution of the DEM, selected because it is the minimum radius needed to calculate slope with this method. The DEM may be passed through a Wiener filter (Wiener, 1949; Robinson and Treitel, 1967) to reduce noise from lidar datasets and/or degraded by averaged subsampling before the determination of slope to match complementary datasets. The effect of enabling these optional treatments is further discussed in the results section. Although methods exist to account for vegetation cover in the DEM (Hladik and Alber, 2012; Wang et al., 2009; Sadro et al., 2007; Chassereau et al., 2011; Montané and Torres, 2006), we chose not to apply these corrections as we wanted to ensure that the TIP method can be applied without information on the vegetation assemblages at a given site.

2.3 Scarp routing

Tidal flats and salt marshes occur mostly on low energy coasts (Allen, 2000), ~~characterized~~ characterised by low local relief and slopes. They therefore display similar local slope values, and this parameter alone is insufficient to differentiate between tidal flats and marsh platforms. Likewise, although marsh platforms are locally higher than tidal flats and channels, this may not be the case for ~~extensive marsh systems~~ complex depositional environments (e.g. marshes sheltered by a sand spit), where

long-shore declivity may cause portions of the tidal flats to be higher than distant emergent platforms. Therefore, elevation alone, though it may be used to visually identify salt marsh platforms, is insufficient for objective platform detection. We address this problem by investigating transition features such as channel banks and erosion scarps, which are outliers in both slope and elevation rasters. These features are commonly defined by steep local slopes, particularly in mature and eroding systems (Defina et al., 2007; Marani et al., 2013). Furthermore, scarps connect marsh platforms to tidal flats, and therefore represent a distinct break in elevation between the two. ~~However, newly formed or seasonal marshes up to the establishment phase of development (Corenblit et al., 2015) have little impact on local topography and will not have formed platforms: they are unlikely to be detected by a topographic method.~~ In this study, we ~~therefore~~ focus on the identification of scarps and steep channel banks as a precursor to the detection of platforms, referred to as step 4 in Fig. 1.

10 To reduce computational costs, we delineate an initial search space to initiate the detection of scarps by isolating steep areas of the landscape, weighted by their elevation. We first calculate the relief of each pixel, R_i ,

$$R_i = z_i - z_{min}, \quad (1)$$

where z_i [dimensions L] is the elevation of the pixel and z_{min} [L] is the minimum elevation in the DEM. We then divide this relief by the maximum relief in the DEM to get a dimensionless relief at each pixel, R_i^* :

$$15 \quad R_i^* = \frac{R_i}{z_{max} - z_{min}} \quad (2)$$

A similar procedure is followed for slope, where Rs [dimensionless] is determined by the slope at a pixel, S_i minus the minimum slope S_{min} :

$$Rs_i = S_i - S_{min}, \quad (3)$$

and the dimensionless version is calculated as:

$$20 \quad Rs_i^* = \frac{Rs_i}{S_{max} - S_{min}} \quad (4)$$

We then multiply these two metrics at each pixel to create the dimensionless parameter P_i^* at each pixel:

$$P_i^* = R_i^* Rs_i^* \quad (5)$$

This dimensionless product is useful for highlighting steep areas at high elevations (Fig. 3): the higher the value of P_i^* , the steeper and higher the pixel is. P_i^* could vary between 0 and 1, where a value of 0 would mean that a pixel was at both the lowest elevation and gradient in the DEM, and vice-versa for a value of 1.

We use the properties of the ~~distribution~~ probability distribution function (pdf) of P^* to define the first search space, which we call Ss_1 . With the exception of macrotidal sites S5 and S6, the pdf of P^* decreases monotonically with increasing P^* , and at sites S5 and S6 the pdf decreases monotonically after a peak value (Fig. 3a). When $f(P^*) < \max(f(P^*))$ and $P^* > \max(P^*)$, the derivative of the pdf is negative and increasing, i.e., the slope of the pdf curve becomes gentler with increasing P^* . We 5 therefore define the threshold value P_{th} where the slope of the pdf is equal to a threshold slope, Sp_{thresh} , on the declining limb of the pdf curve (Fig. 3a). In this study we optimize the threshold value Sp_{thresh} to improve the classification of each site, as described in the Results section. The first search space, Ss_1 , is defined as those pixels where $P^* > P_{th}$, as shown in Fig. 3b. The search space Ss_1 is also schematically represented as grey cells in Fig. 4a (step 4.1)

We then define a square kernel K_3 of 3 cells in width around each cell in Ss_1 . If more than one cell of K_3 is included in Ss_1 , 10 the cell containing the local slope maximum in K_3 is flagged as a first order scarp cell Sc_1 . If one given K_3 already contains an Sc_1 cell that is not the central cell, the central cell will be flagged as an Sc_1 if and only if it is the next local maximum in K_3 . This results in a patchwork of first order scarp cells (step 4.2 in Fig. 4a).

For each first order scarp cell Sc_1 , we then flag two second order cells Sc_2 as ~~neighboring~~ neighbouring cells with the next 15 steepest slopes contained in the search space and not in contact with each other (red outlines in Fig. 4b). If two Sc_1 cells are adjacent, only the cell with the higher slope will be flagged as a Sc_2 cell (step 4.3 in Fig. 4b). This generates a patchwork of first order cells (black outlines Fig. 4b) flanked by one or two second order cells (red outlines in Fig. 4b). Starting from the second order cells Sc_2 , we prolong the scarps by finding the cell with the steepest slope that is not adjacent to another identified 20 scarp cell of two lesser orders, within a K_3 kernel ~~entered~~ centred on the previously identified cell. For example, on the third iteration Sc_3 cells are identified in a K_3 kernel ~~entered~~ centred on a Sc_2 cell and must not be adjacent to an Sc_1 cell. Generally, Sc_n cells are identified in a K_3 kernel ~~entered~~ centred on a Sc_{n-1} cell and must not be adjacent to an Sc_{n-2} cell. This routing 25 procedure is applied in all kernels containing no more than two scarp cells and repeated until no cells fit the conditions or the order n is equal to 100 (blue outlines, step 4.4 in Fig. 4b).

This procedure produces a large number of ~~scars~~ potentially misidentified scarps, as small creeks within the platform and 30 in higher portions of the tidal flat tend to be selected during this procedure. We use a further algorithm to thin these scarps and eliminate creeks. The first procedure eliminates low elevation scarps. We first define a kernel of 9 cells in width K_9 (i.e., a square kernel of 81 pixels with the pixel being interrogated at its ~~enter~~ centre) and compare its maximum elevation $\max(ZK_9)$ to the 75th percentile q_{75} of the entire DEM. Cells that do not satisfy the condition $\max(ZK_9) > ZK_{thresh} \times q_{75}$ are discarded from the finale ensemble of scarps (step 4.5 in Fig. 4c), where ZK_{thresh} is a parameter which we optimize below. Each K_9 kernel containing less than 8 flagged cells is then discarded from the ensemble of scarps; after this procedure finishes we are left with the final ensemble of scarps (step 4.6 in Fig. 4d).

2.4 Platform identification

We identify marsh platforms based on the final ensemble of scarps (step 5 in Fig. 1). The final ensemble of scarps becomes a new search space Ss_2 . We then create a square kernel 3 cells in width (K_3) around each cell in this new search space. Using this kernel we identify first order platform cells, Pc_1 , which are defined as all cells within K_3 that have higher elevation values

than the central cell of the kernel (i.e., those that are higher in elevation than the cells in the final scarp ensemble). We do this because platform cells are located at higher elevations than the scarp cells separating them from tidal flats. We use a kernel rather than a simple blanket elevation threshold over the entire DEM because longitudinal elevation variations may cause some tidal flat cells to be higher than scarp cells. Each Pc_1 cell that is not adjacent to at least 2 other Pc_1 cells is considered a product of isolated situations and eliminated from the ensemble of platform cells.

Following this initial selection of platform cells, we proceed to iteratively fill the platforms. At this point, the initial ensemble of platform cells, Pc_1 , is clustered around the final ensemble of scarps since we have only used a 3 pixel wide kernel ~~entered centred~~ on scarp cells to create the ensemble of Pc_1 cells. We then iterate using a filling algorithm. The first iteration uses the cells Pc_1 , the second Pc_2 , and so on. In each iteration of Pc_n cells, new cells are identified using two kernels, ~~one being larger than the other~~. First, we define a local elevation condition using an 11 pixel wide kernel K_{11} : we find the maximum elevation in this kernel and then subtract 20 cm to define the minimum local elevation for a platform pixel. The 20 cm leeway is applied to account for local elevation variations on the platforms. ~~The algorithm will not identify as separate platforms separated by scarps less than this elevation threshold, so on microtidal marshes this threshold can be lowered. We address this limitation in the discussion and appendix. The threshold is necessary to prevent the algorithm from excluding pools and slight depressions in the platform surface.~~

We then use a 3 pixel wide kernel K_3 within K_{11} to identify any cells in the next iterations' platform ensemble (Pc_{n+1}). These cell must meet two conditions: i) that they are higher than the local elevation threshold identified with the 11 pixel kernel, and ii) that their distance to the nearest cell in the final scarp ensemble is greater than their distance to platform cells from previous iterations. The first condition is simply to ensure the platform is indeed a low relief surface, and the second is to ensure the iterative process fills the platform away from the scarps. The second condition is also necessary to ensure the platform filling process does not cross scarps. This iterative process is repeated until n reaches an arbitrary value of 100, found to be sufficient to fill the entirety of the platform surface area for our sites.

This process results in platforms surfaces that are spatially continuous, but in some instances sections of the tidal flat with relatively high elevations may also have been identified as marsh platforms. These areas are lower than marsh platforms by the height of the scarp separating them. We filter these cells by using the elevation properties of the entire DEM. A number of authors have shown that there is a gap in the probability distribution of elevations in intertidal landscapes that separates the majority of tidal flats from the majority of marsh platforms in micro-tidal environments (e.g., Fagherazzi et al., 2006; Defina et al., 2007; Carniello et al., 2009). Such a separation, demonstrated by the decrease in probability between the grey and blue surfaces in Fig. 5, is also observed in our meso- and macro-tidal sites, including mega-tidal environments such as the Parrett estuary (Fig. 9). We search for this separation using the probability distribution of elevation, $pdf(z)$ of all cells Pc_n , divided in 100 elevations bins. We determine that the most frequent elevation bin $z_{max(pdf(z))}$ is the most likely to contain cells correctly assigned to the platform ensemble, as the relief of marsh platforms is lower than that of tidal flats. Therefore, only elevations lower than $z_{max(pdf(z))}$ may contain cells misidentified as marsh platforms.

We then must identify which cells from the population of cells lower than $z_{max(pdf(z))}$ form part of the platform, and which do not. To do this, we truncate low elevations that have a low probability (See red curves in Fig. 5). ~~If we did not do this we would~~

have a ~~-, to remove the~~ long tail of low elevations from our initial platform identification. We take the probability distribution of the elevation of the remaining platform cells and calculate the mean probability \bar{pdf} (i.e., we average the probability from the 100 bins). We then search for rz_{thresh} consecutive elevation bins that lie below the elevation of the maximum probability elevation that have lower probabilities than this average. The reason we use consecutive bins is that we do not want the 5 minimum elevation to be determined by a single low probability elevation that has spuriously arisen from the binning process. Once we find rz_{thresh} consecutive elevation bins meeting these criteria we remove all cells lower and including the highest cell that lies within the rz_{thresh} consecutive bins. We optimize the parameter rz_{thresh} below.

Having eliminated these low elevation, low probability cells, we also mark all cells higher than $z_{max(f(z))}$ as platform cells. This may still leave pools and ~~pansm~~^{pans} and platform edges remain jagged. Our final procedure aims to eliminate these 10 artifacts using the following procedure: for a given value of the order n , we search in the ensemble of Pc_n cells for cells that are surrounded by more than 6 Pc cells of any order within a K_3 kernel. The 2 or less empty cells in K_3 are then attributed the order $n-1$. By iterating through values of n , starting with the order 100 and finishing with the order 2, we progressively fill pools and 15 jagged borders of the platform (Fig. 6a). Choosing 6 as the minimal number of platforms cells in each K_3 necessary to execute this "reverse filling" procedure, we ensure that no headlands are generated. We then integrate scarp cells that are connected to platform cells into the platform ensemble with an order greater than 100. We then repeat the "reverse filling" process (Fig. 6b) and execute low-elevation elimination procedure (See blue curves in Fig. 5) to obtain the final platform ensemble.

3 Results and discussion

2.1 Performance metrics

In order to evaluate the performance of the TIP method, we compare its outputs to manually ~~digitized~~^{digitised} platforms for 20 all of our test sites (step 7 in Fig. 1). ~~For each grid cell in the detected (automatically processed) and the reference (manually digitised) outputs, we assign the boolean value True to the marsh platform and False to the tidal flat.~~ The results are classified as follows: true positives correspond to matching ~~marsh platform~~^{True} cells in the tested ~~(automatically processed) and reference (manually digitized) and reference~~ outputs, true negatives to matching ~~tidal flats~~^{False} cells, false positives to ~~marsh platforms identified using TIP that are tidal flats in digitized maps~~^{True} cells in the tested output that are False in the reference output, 25 and false negatives ~~where TIP identifies tidal flats in locations that have been digitized as marsh platforms~~^{to False} cells in the tested output that are True in the reference output. The performance of the method is then evaluated using three metrics based on the numbers of true positive (TP), true negative (TN), false positive (FP), and false negative (FN) cells respectively. The accuracy Acc (Fawcett, 2006) describes the likelihood of cells in the tested raster corresponding to the reference raster:

$$Acc = \frac{TP + TN}{TP + TN + FP + FN} \quad (6)$$

We also test the performance of the method by reporting two other metrics: the precision, *Pre*, and the sensitivity, *Sen* (Fawcett, 2006). The precision represents the likelihood of the tested raster overestimating the positives compared to the reference:

$$Pre = \frac{TP}{TP + FP} \quad (7)$$

5 Conversely, the sensitivity *Sen*, represents the likelihood of the tested raster missing positives compared to the reference:

$$Sen = \frac{TP}{TP + FN} \quad (8)$$

If the results of the TIP method perfectly matched that of the manual ~~digitization~~digitisation, all three metrics would have a value of 1.

3 Results

10 3.1 Parameter optimisation

The TIP method contains three user-defined, non-dimensional parameters occurring in sequence during the detection process. The first parameter, Sp_{thresh} , determines the threshold value P^*_{th} for the high-pass filter leading to the selection of the initial search space, shown in Fig. 3a. The parameter Sp_{thresh} influences the solution of the equation $\frac{df}{dP^*} = Sp_{thresh}$. The second parameter, ZK_{thresh} determines the condition on the refinement of existing scarps in the high-pass filter $\max(ZK_9) > 15 ZK_{thresh} \times q_{75}$, schematically represented in Fig. 4. The third parameter, rz_{thresh} is used in the platform dispersion process to determine which percentage of the elevation range below $p\bar{df}$ is maintained in the platform ensemble. In this study, these parameters were set to maximize the average accuracy \bar{Acc} across test sites (Fig. 7): the optimized values ($Sp_{thresh}=-2.0$, $ZK_{thresh}=0.85$, $rz_{thresh}=8$) were used for the subsequent performance analysis. Users may modify these parameters as directed in the code documentation to better fit their study sites.

20 3.2 Performance analysisValidation and applicability

We report Figure 8 shows the performance of the TIP method for all six sites in Fig. 8, discriminating between the use or absence of a Wiener filter and evaluating the influence of progressive resolution degradation how the resolution of the topographic data influences the results. We also provide the full performance metrics in Appendix A (Tables A1 to A6). We find the method's accuracy to be on average of 94.8% at the data's native resolution of 1 m, whether we apply a Wiener filter (Fig. 8a2) or not (Fig. 8a1). This high accuracy signifies that the method can be used to determine the marsh platform extent within 5% of a reference value, as shown in Fig. 11a; this standard is not preserved in perimeter estimates (Fig. 11b). For resolutions of 3 m or less, the accuracy remains on average Degrading the DEM resolution still results in accuracy of above 90% when no

filter is applied, with however a decrease in accuracy and a departure from the 5% buffer in area correspondence in micro- to meso-tidal sites, although it decreases to around 60% for microtidal site S1 and S2 when at a resolution of 3 m. Applying a Wiener filter is applied. We attribute this phenomenon to the more jagged contours of these sites (see Fig. 10a and b), which coarser grids and denoised rasters do not detect. The effect of grid size is also translated in the strong decrease in detected perimeter observed in Fig. 11b; this is because less complex contours lead to shorter boundaries. Such outlines are also more likely to be blurred by the use of a Wiener filter, as demonstrated by the generally lower precision of sites S1 and S2 when using a Wiener filter to the data causes a slight decrease in accuracy and precision (Fig. 8b2). This diminution in precision is compensated by higher average sensitivity values when using a Wiener filter, but an increase in sensitivity (compare Fig. 8c2 to Fig. 8c1). We therefore Examining the results of all of the metrics shows that resolution degradation up to 3 m, well as the use of a Wiener filter, primarily causes an increase in false positives and therefore an overestimation in the extent of the marsh platform. For sites S2 to S6, we observe little change in performance metrics with resolution degradation up to 3 m.

We suggest that all three metrics are used when testing this method on performance metrics should be used when optimising the TIP method for a study site, as no combination of two metrics provides comprehensive insight as to eventual mismatches into TIP uncertainties. Furthermore, although average accuracies remain above 85% for resolutions of 4 to 5 m, we recommend caution when using the method at these resolutions, particularly in micro- to meso-tidal settings where features may be smoothed beyond the method's recognition capacities. Use of the TIP method is not recommended for resolutions coarser than 5m-5 m due to the very low accuracies observed for our test sites, making the TIP this method adapted to high-resolution data sources such as airborne lidar or photogrammetry.

Figures 10 and 9 show how the morphology of the landscapes influences the performance of

20 4 Discussion

4.1 Influence of site morphology on the TIP method

In order to examine the performance of the method in sites with varying morphological characteristics, we compare the probability distribution functions (pdf) of elevation from the digitised platforms to the platforms detected using the TIP method. Figure 10a shows that in micro-tidal environments, the method tends to overestimate the extent of the marsh platform (seen as false positives), as is confirmed by the higher peak probability of detected platforms as well as the low-elevation abrupt tail shown (Fig. 9). Figures 9a to f show that a left-hand tail is present for the digitised platforms, whereas platforms detected by TIP show a sharp decrease in the pdf at these elevations: this indicates the presence of more false negatives than false positives at the lowest elevations of the marsh platform. This suggests that the TIP method excludes more features with a low elevation than manual digitisation, which correspond to tidal creeks and sunken terraces at the edge of the platform. However, this does not imply that the TIP method cannot identify multiple terraces within a platform, as shown by the multiple local maxima in the detected pdf in Fig. 9ad and f.

We also show maps of the TIP method's performance for each test site in order to explore this spatial variability in feature detection (Fig. 10). For instance, the dominance of false positives over false negatives in Fig. 10a (site S1) suggests that the

method tends to overestimate the extent of jagged, low-relief marsh platforms, which are common in the sheltered microtidal bays characterising this site. This is the product of two ~~combined~~ factors: (i) identified scarps are not always complete in micro-tidal ~~environmental where scarps are small and more liable to sub-threshold elimination environments, as scarps tend to be small and therefore liable to elimination by our elevation threshold~~ (see Fig. 4, step 4.5); and (ii) the reverse dispersion process (see Fig. 6) is then likely to encroach on the tidal flat, ~~generating a high number of false positives (see the high left-hand tail in Fig. 9a)~~. This process is different from the generation of false positives in ~~9~~. This phenomenon is exacerbated by coarse grids or de-noised datasets (e.g. Fig. 8a1 and a2) where high slope values are smoothed and filtered out in the scarp detection process. In our meso- to macro-tidal sites S2 to S4 (Fig. 10e-f, although the sharp cut-off at the lowest tail of b-d), the ~~elevation distribution~~ method results in false negatives corresponding to the location of tidal creeks. These creeks were purposefully included in the marsh platform during the digitisation process, but were identified as part of the tidal flat by the TIP method. This result indicates that our method often characterises creek banks as platform scarps due to their morphological similarity.

Other coastal landforms may generate false positives, as seen in Fig. 9~~does not show this difference~~ 10 c-f. In these cases, the position of the scarp line differs between the ~~digitized~~ ~~digitised~~ and the TIP-detected platforms due to elevated portions of the tidal flat being ~~back-to-back with adjacent to~~ the marsh platform. This suggests that some areas of the tidal flat are topographically closer to the platform than to the rest of the tidal flat and may represent areas likely to be ~~colonized~~ ~~colonised~~ by pioneer vegetation, ~~even though they might not be vegetated at the time of data acquisition~~. Conversely, sunken platforms (~~also called saltings in mega-tidal environments where they may be small and numerous~~) or fallen blocks that are not delineated by scarps may generate false negatives, as seen in the central area of Fig. 10e. ~~Most false negatives are however generated by a stricter elimination of tidal creeks by~~

20 Although the TIP method was tested using salt marshes located in England, the scarp and platform association is a common feature to many salt marshes around the world, making the TIP method applicable over a wide range of geographic areas. Furthermore, the TIP method does not require the precise topography of the platform to function, making it relatively insensitive to unequal removal of vegetation between different DEM sources. The presence of vegetation induces positive errors in the DEM, which counter-intuitively may be useful when applying the TIP method, as this artificially increases the platform height
25 and therefore the scarp slope. Examples of sites outside the United Kingdom are included in Fig. B2, and were selected to demonstrate the versatility but also the limits of the TIP method.

4.2 Future developments

As discussed in Section 4.1, the TIP method currently excludes tidal creeks from the marsh platform, leading to discrepancies when compared to manual digitisation. Therefore, we would expect the TIP method ~~than by manual digitization, a trait particularly visible in Fig. 10b and d. This result confirms that topographic analyses of coastal marshes require a simultaneous analysis to underperform on highly dissected marsh platforms. As a proxy for the dissection of the platform by tidal creeks, we digitise tidal creek centrelines from the DEM. We then calculate the total length of tidal creeks included in the digitised platform divided by the platform surface area. We refer to this quantity as the Dissection Index (DI). In Fig. 11, we examine the capacity of the TIP-method to determine the area and perimeter of marsh platforms according to their dissection index.~~

We find that for all test sites, TIP-detected area remains within 10% of the digitised area, whereas TIP-detected perimeter increases steadily with Dissection Index, confirming that the exclusion of tidal creeks, which can be identified from lidar data using established by the TIP method is consistently stricter than by digitisation. However, neither the TIP method nor manual digitisation offer an objective solution to detect tidal creeks. For a comprehensive analysis of marsh platforms, we recommend 5 that objective platform detection be used in conjunction with objective creek detection methods such as those of developed by Fagherazzi et al. (1999) and Liu et al. (2015). Fig. 10c also demonstrates that accreting meander banks may be correctly located in large channels, while sand bars inside these channels are correctly excluded from the platform ensemble. This indicates 10 that the use of creek detection methods, while adding an element to topographic analyses, is unlikely to affect the platform properties. Furthermore, future developments of the TIP method will include an objective creek detection method adapted from these publications, as well as channel network extraction methods developed for fluvial channels by Clubb et al. (2014), to 15 ensure that tidal creeks are detected as separate objects.

The morphological characteristics of prograding marshes are different from those of established platforms: consequently, 20 vegetation patches and pioneer zones are not the object of the TIP method. Specifically, prograding margins and vegetation patches tend to have a relief and slope that are close to those of the tidal flat, making their outlines invisible to the scarp routing process. The combined absence of scarp and low relief of prograding marshes then interfere with the 20 cm leeway included in the platform filling process and cause an excess of false positives. Users may reduce this leeway to improve accuracy (see Fig. B2b1), but we discourage the use of the TIP method to identify vegetation patches and prograding margins. However, these 25 dynamic features are the centrepiece of salt marsh development and would benefit from reproducible monitoring methods. Future research may build on the works of Balke et al. (2012) to determine characteristic morphologies of prograding marshes, 30 thus providing the necessary groundwork to enable reproducible monitoring.

4.3 Potential for operational monitoring

As well as providing us with the ability to automate the delineation and analysis of marsh platforms across multiple sites, our 25 method also allows the objective detection of change in marsh extent through time, with important implications for habitat monitoring or carbon storage evaluation. We test the capacity of the TIP method to monitor temporal change through the example of site S6, which was affected by heavy rainfall in the summer of 2007. Rivers 2007, resulting in high discharge in rivers such as the Parrett carried high discharges, and 1 m lidar data distributed by the Environment Agency shows that 30 between March and October 2007 the North-Eastern corner of site S6 underwent significant erosion. Blue pixels indicating loss of elevation (between March and October) in Fig. 12a bear the characteristic shape of slope failures and intersect the both the automatically- and manually-detected platform outline of March 2007 detected both automatically and manually, indicating showing that the October platform outline should be is further inland.

This retreat of the marsh platform is observed both by the objectively classified (Fig. 12b) and the manually digitized digitised platforms (Fig. 12c). However, whereas the digitization digitisation effort focuses on the large bank failures, the TIP method also detects small changes in the DEM at the platform margin (visible in Fig. 12a and b), and may detect them as changes in marsh platform extent. Consequently, despite a close correspondence between TIP-determined marsh outlines and

~~digitized~~ digitised outlines (Fig. 12a) near the bank failures, the ~~digitized~~ digitised volume loss is only 81% of the objectively detected volume loss. Pioneer zones, characterized by shallow slopes and rapid, uneven elevation changes, are also likely to generate small topographic differences between the DEMs.

5 Conclusions

5 In this study we have presented a novel method which uses the topographic signature of salt marsh platforms to determine their seaward extent on high resolution DEMs. By combining non-dimensional search parameters and empirical calibration, it separates marsh platforms from tidal flats with over 90% accuracy for source data of up to 3 m in grid resolution, a result sufficient to allow quantitative morphology analyses and monitoring, particularly for eroding marshes where scarps are clearly defined. Independence from environmental variables means that our method can be used to complement spectral data for identifying plant types, to better understand feedbacks between sedimentation, deposition and biomass. We tested our method on 10 six sites with a wide range of spring tidal ranges and found that tidal range has no significant impact on the detection accuracy. Furthermore, the presence of algae ~~kelp or duckweed~~ as well as varying vegetation ~~characteristics~~ reflectance properties, which may ~~require induce~~ specific calibrations with spectral methods (Morris et al., 2005), do not affect our results (barring mounds of stranded algae large enough to affect topography). Although we did not test the performance of the TIP method 15 on DEM resolutions finer than 1 m, the option of applying a Wiener filter to reduce DEM noise is available to accommodate DEMs generated from unclassified point clouds, which ~~display~~ have higher surface roughness. When combined with creek detection methods ~~such as those proposed by Liu et al. (2015)~~, we expect the performance of the TIP method to improve ~~due to the reduction of~~ with fewer false negatives. This would also allow the discrimination of channel evolution within the marsh platform and on the tidal flat, allowing us to simultaneously explore the development of marsh platforms and tidal creeks 20 (D'Alpaos et al., 2007, 2010) in sites with strong tidal forcing.

Furthermore, the unsupervised detection of marsh platforms from their topography alone reduces the computational cost 25 of topographic analysis compared to spectral studies. This promotes the consideration of salt marshes as topographic objects as well as ecological systems, facilitating holistic, data-driven studies on salt marsh eco-geomorphic responses, and testing existing models of eco-geomorphic feedback (e.g. Fagherazzi et al., 2012). It also encourages us to think of the topographic object separately from the ecological system: mismatches in their respective boundaries may therefore be used to investigate accretion processes and pioneer zone growth in continuation with the works of Balke et al. (2014) and Hu et al. (2015). The examination of such processes at smaller scales, such as those obtained with terrestrial lidar stations, may also reveal 30 characteristic accretion patterns (Balke et al., 2012) which topographic methods may objectively detect. Other developments of this method may, in time, enable the detection of the spatial extent of other ecosystems, such as riparian wetlands and mangrove limits.

Code and data availability. Our software is freely available for download on GitHub as part of the Edinburgh Land Surface Dynamics Topographic Tools package at <https://github.com/LSDtopotools>. The software used in this study is available in this release: https://github.com/LSDtopotools/LSDTopoTools_MarshPlatform/releases/tag/v0.2 (Goodwin et al., 2017).

Author contributions. GCHG designed the method with contributions from other authors. GCHG wrote the code and produced the figures, 5 with support from SMM and FJC in integrating methods with existing channel extraction and topographic processing algorithms. GCHG wrote the paper with contributions from other authors.

Competing interests. The authors declare no competing interests.

Acknowledgements. GCHG was supported by a NERC doctoral training partnership grant (NE/L002558/1). SMM was supported by the Leverhulme Foundation (IAF-2014-009). FJC was supported by NERC grant NE/P012922/1. The authors acknowledge the United Kingdom 10 Environment Agency for the consequent amount of lidar data (point cloud and gridded) made freely available through their website. The authors thank Dr. Dimitri Lague for his insightful comments.

References

Allen, J. R. L.: Morphodynamics of Holocene salt marshes: A review sketch from the Atlantic and Southern North Sea coasts of Europe, *Quaternary Science Reviews*, 19, 1155–1231, doi:10.1016/S0277-3791(99)00034-7, 2000.

Balke, T., Klaassen, P. C., Garbutt, A., Van der Wal, D., Herman, P. M. J., and Bouma, T. J.: Conditional outcome of ecosystem engineering: A case study on tussocks of the salt marsh pioneer *Spartina anglica*, *Geomorphology*, 153-154, 232–238, doi:10.1016/j.geomorph.2012.03.002, 2012.

Balke, T., Herman, P. M. J., and Bouma, T. J.: Critical transitions in disturbance-driven ecosystems: Identifying Windows of Opportunity for recovery, *Journal of Ecology*, pp. 700–708, doi:10.1111/1365-2745.12241, 2014.

Belluco, E., Camuffo, M., Ferrari, S., Modenese, L., Silvestri, S., Marani, A., and Marani, M.: Mapping salt-marsh vegetation by multispectral and hyperspectral remote sensing, *Remote Sensing of Environment*, 105, 54–67, doi:10.1016/j.rse.2006.06.006, 2006.

Carniello, L., Defina, A., and D'Alpaos, L.: Morphological evolution of the Venice lagoon: Evidence from the past and trend for the future, *Journal of Geophysical Research: Earth Surface*, 114, 1–10, doi:10.1029/2008JF001157, 2009.

Chassereau, J. E., Bell, J. M., and Torres, R.: A comparison of GPS and lidar salt marsh DEMs, *Earth Surface Processes and Landforms*, 36, 1770–1775, doi:10.1002/esp.2199, 2011.

Chmura, G. L., Anisfeld, S. C., Cahoon, D. R., and Lynch, J. C.: Global carbon sequestration in tidal, saline wetland soils, *Global Biogeochemical Cycles*, 17, 12, doi:1111 10.1029/2002gb001917, 2003.

Clubb, F. J., Mudd, S. M., Milodowski, D. T., Hurst, M. D., and Slater, L. J.: Objective extraction of channel heads from high-resolution topographic data, *Water Resources Research*, pp. 4840–4847, doi:10.1002/2015WR017273. Received, 2014.

Corenblit, D., Baas, A., Balke, T., Bouma, T., Fromard, F., Garfano-Gómez, V., González, E., Gurnell, A. M., Hortobágyi, B., Julien, F., Kim, D., Lambs, L., Stallins, J. A., Steiger, J., Tabacchi, E., and Walcker, R.: Engineer pioneer plants respond to and affect geomorphic constraints similarly along water-terrestrial interfaces world-wide, *Global Ecology and Biogeography*, 24, 1363–1376, doi:10.1111/geb.12373, 2015.

Costanza, R., Arge, R., Groot, R. D., Farberk, S., Grasso, M., Hannon, B., Limburg, K., Naeem, S., O'Neill, R. V., Paruelo, J., Raskin, R. G., Suttonkk, P., and van den Belt, M.: The value of the world's ecosystem services and natural capital, *Nature*, 387, 253–260, doi:10.1038/387253a0, 1997.

Coverdale, T. C., Brisson, C. P., Young, E. W., Yin, S. F., Donnelly, J. P., and Bertness, M. D.: Indirect human impacts reverse centuries of carbon sequestration and salt marsh accretion, *PLoS ONE*, 9, 1–7, doi:10.1371/journal.pone.0093296, 2014.

Crosby, S. C., Sax, D. F., Palmer, M. E., Booth, H. S., Deegan, L. A., Bertness, M. D., and Leslie, H. M.: Salt marsh persistence is threatened by predicted sea-level rise, *Estuarine, Coastal and Shelf Science*, 181, 93–99, doi:10.1016/j.ecss.2016.08.018, 2016.

D'Alpaos, A., Lanzoni, S., Marani, M., Bonometto, A., Cecconi, G., and Rinaldo, A.: Spontaneous tidal network formation within a constructed salt marsh: Observations and morphodynamic modelling, *Geomorphology*, 91, 186–197, doi:10.1016/j.geomorph.2007.04.013, 2007.

D'Alpaos, A., Lanzoni, S., Marani, M., and Rinaldo, A.: On the tidal prism-channel area relations, *Journal of Geophysical Research: Earth Surface*, 115, 1–13, doi:10.1029/2008JF001243, 2010.

Day, J. W., Britsch, L. D., Hawes, S. R., Shaffer, G. P., Reed, D. J., Cahoon, D., Britsch, L. D., Reed, D. J., Hawes, S. R., and Cahoon, D.: Pattern and process of land loss in the Mississippi Delta: A spatial and temporal analysis of wetland habitat change, *Estuaries*, 23, 425, doi:10.2307/1353136, 2000.

Defina, A., Carniello, L., Fagherazzi, S., and D'Alpaos, L.: Self-organization of shallow basins in tidal flats and salt marshes, *Journal of Geophysical Research: Earth Surface*, 112, 1–11, doi:10.1029/2006JF000550, 2007.

Duarte, C. M., Dennison, W. C., Orth, R. J. W., and Carruthers, T. J. B.: The charisma of coastal ecosystems: Addressing the imbalance, *Estuaries and Coasts*, 31, 233–238, doi:10.1007/s12237-008-9038-7, 2008.

5 Fagherazzi, S., Bortoluzzi, A., Dietrich, W. E., Adamo, A., Lanzoni, S., Marani, M., and Rinaldo, A.: Tidal networks 1. Automatic network extraction and preliminary scaling features from digital terrain maps, *Water Resources Research*, 35, 3891–3904, doi:10.1029/1999WR900236, 1999.

Fagherazzi, S., Carniello, L., D'Alpaos, L., and Defina, A.: Critical bifurcation of shallow microtidal landforms in tidal flats and salt marshes, *Proceedings of the National Academy of Sciences*, 103, 8337–8341, doi:10.1073/pnas.0508379103, 2006.

10 Fagherazzi, S., Kirwan, M. L., Mudd, S. M., Guntenspergen, G. R., Temmerman, S., Rybczyk, J. M., Reyes, E., Craft, C., and Clough, J.: Numerical models of salt marsh evolution: Ecological, geomorphic, and climatic factors, *Review of Geophysics*, 50, 1–28, doi:10.1029/2011RG000359, 2012.

Fawcett, T.: An introduction to ROC analysis, *Pattern Recognition Letters*, 27, 861–874, doi:10.1016/j.patrec.2005.10.010, 2006.

Feagin, R. A., Martinez, M. L., Mendoza-Gonzalez, G., and Costanza, R.: Salt marsh zonal migration and ecosystem service change in 15 response to global sea level rise: A case study from an urban region, *Ecology & Society*, 15, 1–15, <http://www.ecologyandsociety.org/vol15/iss4/art14/>, 2010.

Goodwin, G. C. H., Mudd, S. M., and Clubb, F. J.: LSDtopotools Marsh Platform Identification Tool, Tech. rep., Zenodo, doi:10.5281/zenodo.1007788, 2017.

Grieve, S. W. D., Mudd, S. M., Milodowski, D. T., Clubb, F. J., and Furbish, D. J.: How does grid-resolution modulate the topographic 20 expression of geomorphic processes?, *Earth Surface Dynamics*, 4, 627–653, doi:10.5194/esurf-4-627-2016, 2016.

Hladik, C. and Alber, M.: Accuracy assessment and correction of a LIDAR-derived salt marsh digital elevation model, *Remote Sensing of Environment*, 121, 224–235, doi:10.1016/j.rse.2012.01.018, 2012.

Hladik, C. and Alber, M.: Classification of salt marsh vegetation using edaphic and remote sensing-derived variables, *Estuarine, Coastal and Shelf Science*, 141, 47–57, doi:10.1016/j.ecss.2014.01.011, 2014.

25 Hladik, C., Schalles, J., and Alber, M.: Salt marsh elevation and habitat mapping using hyperspectral and LIDAR data, *Remote Sensing of Environment*, 139, 318–330, doi:10.1016/j.rse.2013.08.003, 2013.

Hu, Z., Van Belzen, J., Van Der Wal, D., Balke, T., Wang, Z. B., Stive, M., and Bouma, T. J.: Windows of opportunity for salt marsh vegetation establishment on bare tidal flats: The importance of temporal and spatial variability in hydrodynamic forcing, *Journal of Geophysical Research G: Biogeosciences*, 120, 1450–1469, doi:10.1002/2014JG002870, 2015.

30 Hurst, M. D., Mudd, S. M., Walcott, R., Attal, M., and Yoo, K.: Using hilltop curvature to derive the spatial distribution of erosion rates, *Journal of Geophysical Research: Earth Surface*, 117, 1–19, doi:10.1029/2011JF002057, 2012.

Jucke van Beijma, S.: Remote Sensing - Based Mapping and Modelling of Coastal Salt Marsh Habitats Based on Optical , Lidar and SAR Data. Thesis submitted for the degree of Doctor of Philosophy at the University of Leicester, Ph.D. thesis, 2015.

Kirwan, M. and Temmerman, S.: Coastal marsh response to historical and future sea-level acceleration, *Quaternary Science Reviews*, 28, 35 1801–1808, doi:10.1016/j.quascirev.2009.02.022, <http://dx.doi.org/10.1016/j.quascirev.2009.02.022>, 2009.

Kirwan, M. L. and Megonigal, J. P.: Tidal wetland stability in the face of human impacts and sea-level rise., *Nature*, 504, 53–60, doi:10.1038/nature12856, 2013.

Kirwan, M. L., Murray, A. B., Donnelly, J. P., and Corbett, D. R.: Rapid wetland expansion during European settlement and its implication for marsh survival under modern sediment delivery rates, *Geology*, 39, 507–510, doi:10.1130/G31789.1, 2011.

Leonardi, N. and Fagherazzi, S.: How waves shape salt marshes, *Geology*, 42, 887–890, doi:10.1130/G35751.1, 2014.

Liu, Y., Zhou, M., Zhao, S., Zhan, W., Yang, K., and Li, M.: Automated extraction of tidal creeks from airborne laser altimetry data, *Journal of Hydrology*, 527, 1006–1020, doi:10.1016/j.jhydrol.2015.05.058, 2015.

Marani, M., D'Alpaos, A., Lanzoni, S., Carnielo, L., and Rinaldo, A.: Biologically-controlled multiple equilibria of tidal landforms and the fate of the Venice lagoon, *Geophysical Research Letters*, 34, 1–5, doi:10.1029/2007GL030178, 2007.

Marani, M., Da Lio, C., and D'Alpaos, A.: Vegetation engineers marsh morphology through multiple competing stable states., *Proceedings of the National Academy of Sciences of the United States of America*, 110, 3259–63, doi:10.1073/pnas.1218327110, 2013.

Mo, Y., Momen, B., and Kearney, M. S.: Quantifying moderate resolution remote sensing phenology of Louisiana coastal marshes, *Ecological Modelling*, 312, 191–199, doi:<http://dx.doi.org/10.1016/j.ecolmodel.2015.05.022>, 2015.

Moffett, K. B., Robinson, D. A., and Gorelick, S. M.: Relationship of Salt Marsh Vegetation Zonation to Spatial Patterns in Soil Moisture, Salinity, and Topography, *Ecosystems*, 13, 1287–1302, doi:10.1007/s10021-010-9385-7, 2010.

Moffett, K. B., Gorelick, S. M., McLaren, R. G., and Sudicky, E. A.: Salt marsh ecohydrological zonation due to heterogeneous vegetation-groundwater-surface water interactions, *Water Resources Research*, 48, doi:10.1029/2011WR010874, 2012.

Möller, I. and Spencer, T.: Wave dissipation over macro-tidal saltmarshes: Effects of marsh edge typology and vegetation change, *Journal of Coastal Research*, 36, 506–521, doi:ISSN:0749-0208, 2002.

Montané, J. M. and Torres, R.: Accuracy Assessment of Lidar Saltmarsh Topographic Data Using RTK GPS, *Photogrammetric Engineering & Remote Sensing*, pp. 961–967, doi:0099-1112/06/7208-0961, 2006.

Morris, J. T., Sundareshwar, P. V., Nietch, C. T., Kjerfve, B., and Cahoon, D. R.: Responses of Coastal Wetlands to Rising Sea Level, *Ecology*, 83, 2869–2877, doi:10.1890/0012-9658(2002)083[2869:ROCWTR]2.0.CO;2, 2002.

Morris, J. T., Porter, D., Neet, M., Noble, P. a., Schmidt, L., Lapine, L. a., and Jensen, J. R.: Integrating LIDAR elevation data, multi-spectral imagery and neural network modelling for marsh characterization, *International Journal of Remote Sensing*, 26, 5221–5234, doi:10.1080/01431160500219018, 2005.

Mudd, S. M., Fagherazzi, S., Morris, J. T., and Furbish, D. J.: Flow, sedimentation, and biomass production on a vegetated salt marsh in South Carolina: toward a predictive model of marsh morphologic and ecologic evolution, *American Geophysical Union*, pp. 165–187, doi:10.1029/CE059p0165, 2004.

Mudd, S. M., Howell, S. M., and Morris, J. T.: Impact of dynamic feedbacks between sedimentation, sea-level rise, and biomass production on near-surface marsh stratigraphy and carbon accumulation, *Estuarine, Coastal and Shelf Science*, 82, 377–389, doi:10.1016/j.ecss.2009.01.028, 2009.

Mudd, S. M., D'Alpaos, A., and Morris, J. T.: How does vegetation affect sedimentation on tidal marshes? Investigating particle capture and hydrodynamic controls on biologically mediated sedimentation, *Journal of Geophysical Research: Earth Surface*, 115, doi:10.1029/2009JF001566, 2010.

Nardin, W. and Edmonds, D. A.: Optimum vegetation height and density for inorganic sedimentation in deltaic marshes, *Nature Geoscience*, 7, 722–726, doi:10.1038/ngeo2233, 2014.

Nelson, J. L. and Zavaleta, E. S.: Salt marsh as a coastal filter for the oceans: Changes in function with experimental increases in Nitrogen loading and sea-level rise, *PLoS ONE*, 7, doi:10.1371/journal.pone.0038558, 2012.

Pennings, S. C., Grant, M. B., and Bertness, M. D.: Plant zonation in low-latitude salt marshes: Disentangling the roles of flooding, salinity and competition, *Journal of Ecology*, 93, 159–167, doi:10.1111/j.1365-2745.2004.00959.x, 2005.

Reed, D. and Cahoon, D.: The relationship between marsh surface topography, hydroperiod, and growth of *Spartina alterniflora* in a deteriorating Louisiana salt marsh, *Journal of Coastal Research*, 8, 77–87, www.jstor.org/stable/4297954, 1992.

5 Robinson, E. A. and Treitel, S.: Principles of Digital Wiener Filtering, *Geophysical Prospecting*, 15, 311–332, doi:10.1111/j.1365-2478.1967.tb01793.x, 1967.

Sadro, S., Gastil-Buhl, M., and Melack, J.: Characterizing patterns of plant distribution in a southern California salt marsh using remotely sensed topographic and hyperspectral data and local tidal fluctuations, *Remote Sensing of Environment*, 110, 226–239, doi:10.1016/j.rse.2007.02.024, 2007.

10 Schroder, A., Persson, L., de Roos, A. M., and Lundbery, P.: Direct Experimental Evidence for Alternative Stable States: A Review, *Oikos*, 110, 3–19, doi:10.1111/j.0030-1299.2005.13962.x, 2005.

Shepard, C. C., Crain, C. M., and Beck, M. W.: The protective role of coastal marshes: A systematic review and meta-analysis, *PLoS ONE*, 6, doi:10.1371/journal.pone.0027374, 2011.

Silvestri, S., Marani, M., and Marani, A.: Hyperspectral remote sensing of salt marsh vegetation, morphology and soil topography, *Physics and Chemistry of the Earth*, 28, 15–25, doi:10.1016/S1474-7065(03)00004-4, 2003.

15 Temmerman, S., Bouma, T. J., Van de Koppel, J., Van der Wal, D., De Vries, M. B., and Herman, P. M. J.: Vegetation causes channel erosion in a tidal landscape, *Geology*, 35, 631–634, doi:10.1130/G23502A.1, 2007.

Tuxen, K. A., Schile, L. M., Kelly, M., and Siegel, S. W.: Vegetation colonization in a restoring tidal marsh: A remote sensing approach, *Restoration Ecology*, 16, 313–323, doi:10.1111/j.1526-100X.2007.00313.x, 2008.

20 Wang, C., Menenti, M., Stoll, M. P., Belluco, E., and Marani, M.: Mapping mixed vegetation communities in salt marshes using airborne spectral data, *Remote Sensing of Environment*, 107, 559–570, doi:10.1016/j.rse.2006.10.007, 2007.

Wang, C., Menenti, M., Stoll, M. P., Feola, A., Belluco, E., and Marani, M.: Separation of ground and low vegetation signatures in LiDAR measurements of salt-marsh environments, *IEEE Transactions on Geoscience and Remote Sensing*, 47, 2014–2023, doi:10.1109/TGRS.2008.2010490, 2009.

25 Wiener, N.: Extrapolation, interpolation, and smoothing of stationary time series: with engineering applications, *Technology Press of the Massachusetts Institute of Technology*, 1949.

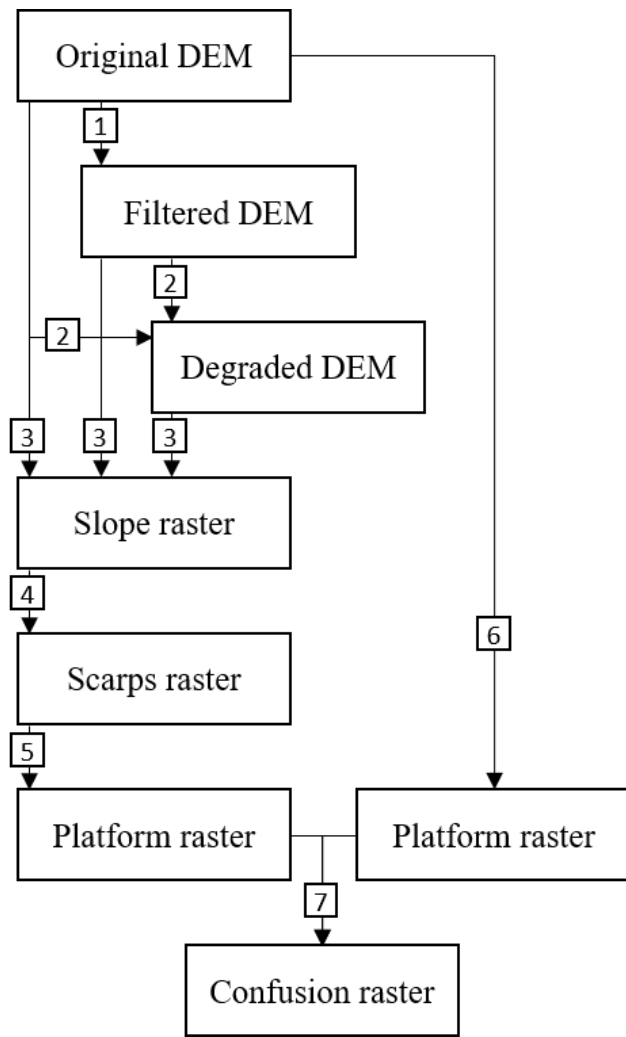


Figure 1. Flow chart showing the overall structure of the TIP method and its validation. Each object (rectangle) is obtained by implementing a routine (square), numbered as follows: 1. Implementation of a Wiener filter (optional); 2. Subsampling by average value (optional); 3. Calculation of slope by fitting a second order polynomial surface; 4. Scarp identification by routing; 5. Platform identification by dispersion; 6. Manual ~~digitization~~ ~~digitisation~~ of a marsh platform; 7. Comparison of the objectively detected platform to the manually ~~digitized~~ ~~digitised~~ platform.

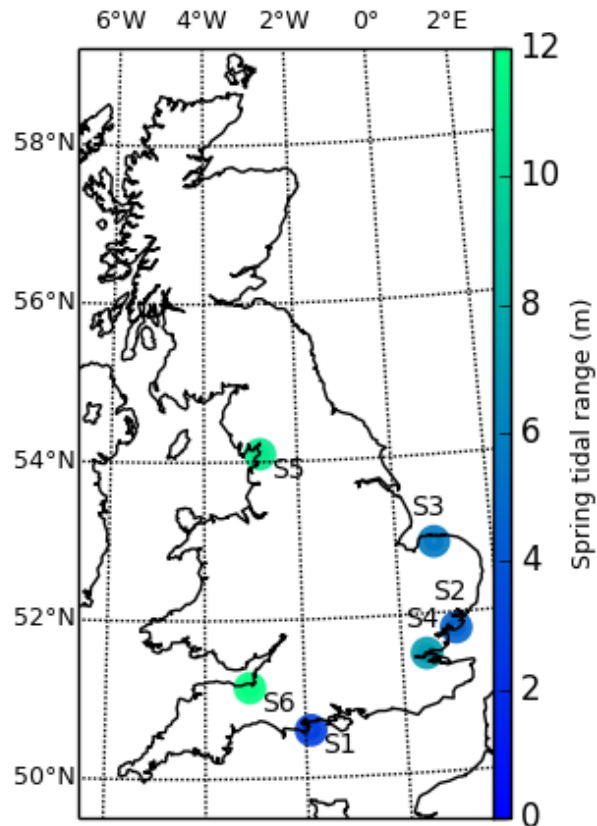


Figure 2. This map shows the six sites selected from the lidar collection of the UK environment agency, [colored](#) by spring tidal range. The sites are numbered as follows: S1: Shell Bay, Dorset; S2: Stour Estuary, Suffolk; S3: Stiffkey, Norfolk; S4: Medway Estuary, Kent; S5: Jenny Brown's Point, Lancashire; S6: Parrett Estuary, Somerset.

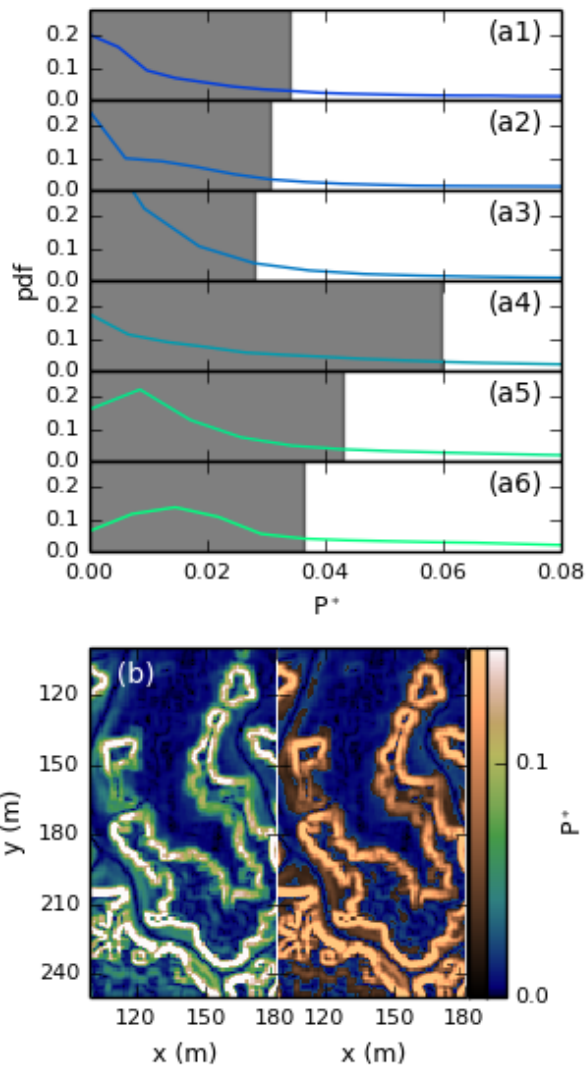


Figure 3. a1-6. Frequency distribution of P^* for sites S1-6. The greyed portion of the plot represents pixels that are not included in the [initial](#) search space Ss_I ; b. raster representation of P^* for site S1: Shell Bay. Values of P^* under P^*_{th} use the topographic [eolor](#)-[colour](#) scheme, while values above P^*_{th} use the copper [eolor](#)-[colour](#) scheme and are included in Ss_I .

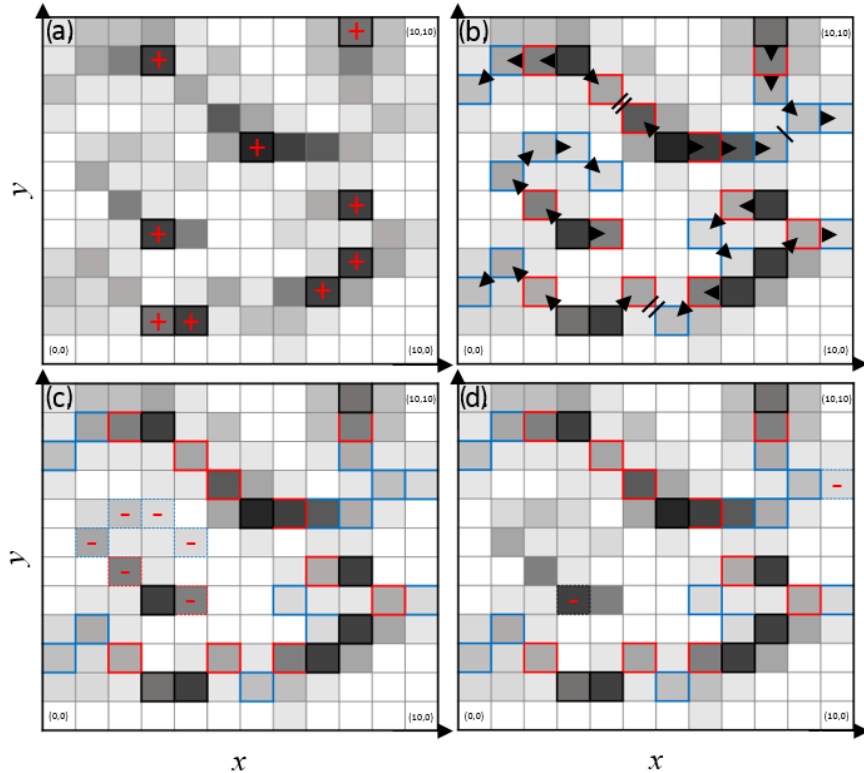


Figure 4. Schematic example of the scarp detection process through maximum slope routing. Panel a. shows two steps. Step 4.1: determination of the search space Ss_1 (greyed cells, darker with arbitrary slope). Step 4.2: Determination of local maxima Sc_1 (black outlines with a plus sign); b. Step 4.3: Determination of Sc_2 cells (red outlines). Step 4.4: Determination of Sc_n cells, $n > 2$ (blue outlines); c. Step 4.5: Elimination of cells where $\max(Zk_9) < 0.85 \times q_{75}$ (dashed outlines with a minus sign); d. Step 4.6: Elimination of isolated cells (dashed outlines with a minus sign). The arrows represent the progressive selection of scarp cells.

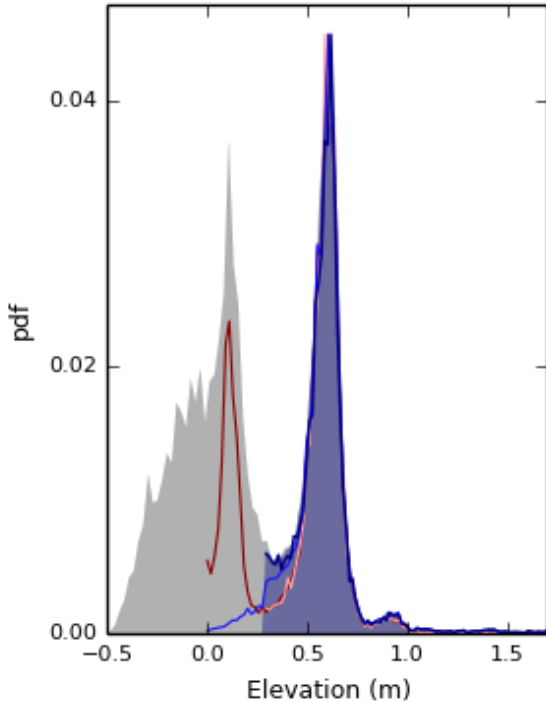


Figure 5. Diagram describing the elimination of the tail of the elevation probability distribution function for site S1. The grey filled surface is the pdf of elevation for the original DEM. The dark red line is the pdf of elevation of the platform after the dispersion process. The orange line is the pdf of elevation of the platform after truncation of the tail of the distribution. The blue line is the pdf of elevation of the platform after filling pools and jagged outlines and after the addition of scarps in the platform ensemble. The dark blue line, associated to the blue filled surface, is the pdf of elevation for the final platform, after the tail of its distribution is truncated a second time. All distributions in this plot ~~were~~are forced to display the same maximum for clarity.

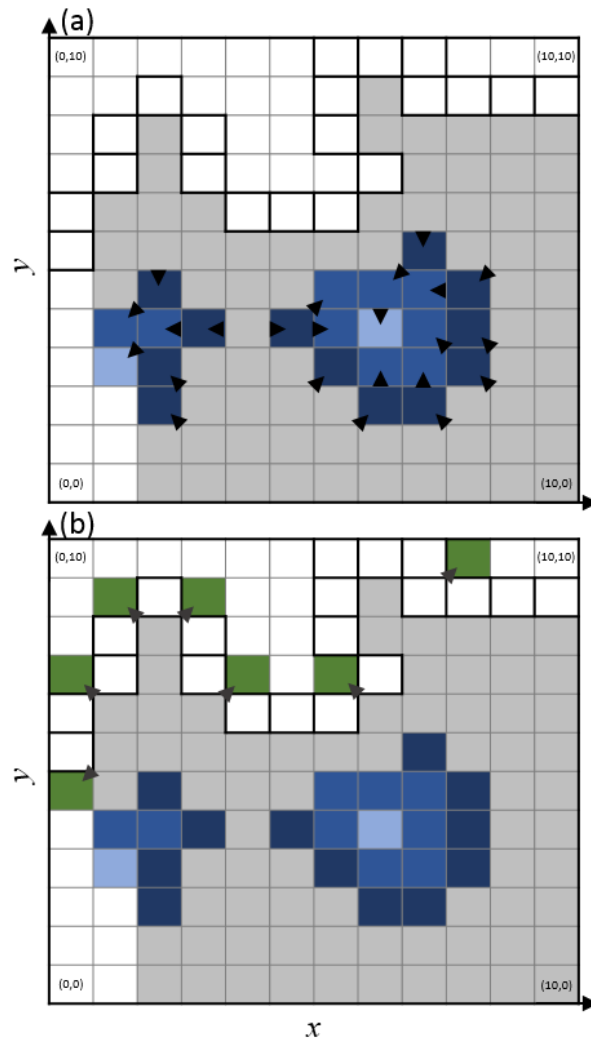


Figure 6. Schematic example of the reverse platform filling process. a. Step 5.1: Filling of empty cells adjacent to P_{C_n} cells (grey, dark blue and blue cells) with and order $n-1$ (dark blue, blue and light blue cells); b. Step 5.2: Filling of empty cells adjacent to P_{C_n} cells (grey cells) with and order $n-1$ (green cells) when scarp cells (black outlines) are included in the platform ensemble. The arrows indicate the dispersion pattern.

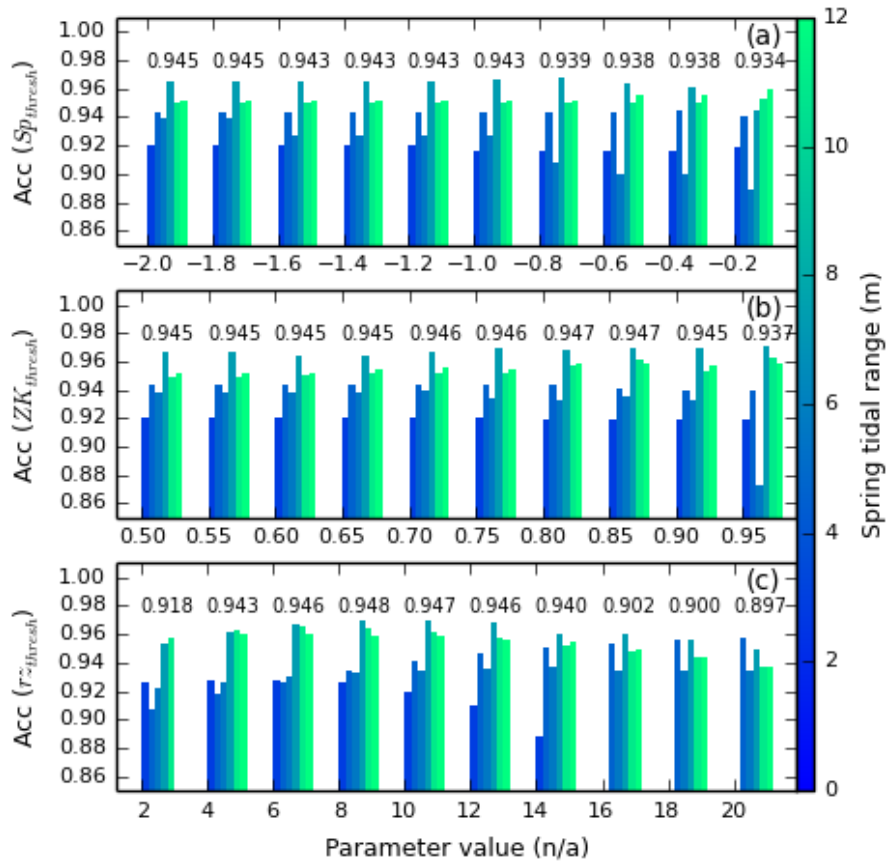


Figure 7. Accuracy charts used to optimize the three user-defined parameters for the six test sites, each site being ~~colored~~^{coloured} by spring tidal range, with no filter. Each group of bars represents the accuracy for one parameter value when applied to all the test sites. The mean accuracy appears above each group; a. Accuracy for the parameter Opt1. The retained value for Opt1 is -2.0; b. Accuracy for the parameter Opt2. The retained value for Opt2 is 0.85; c. Accuracy for the parameter Opt3. The retained value for Opt3 is 8.

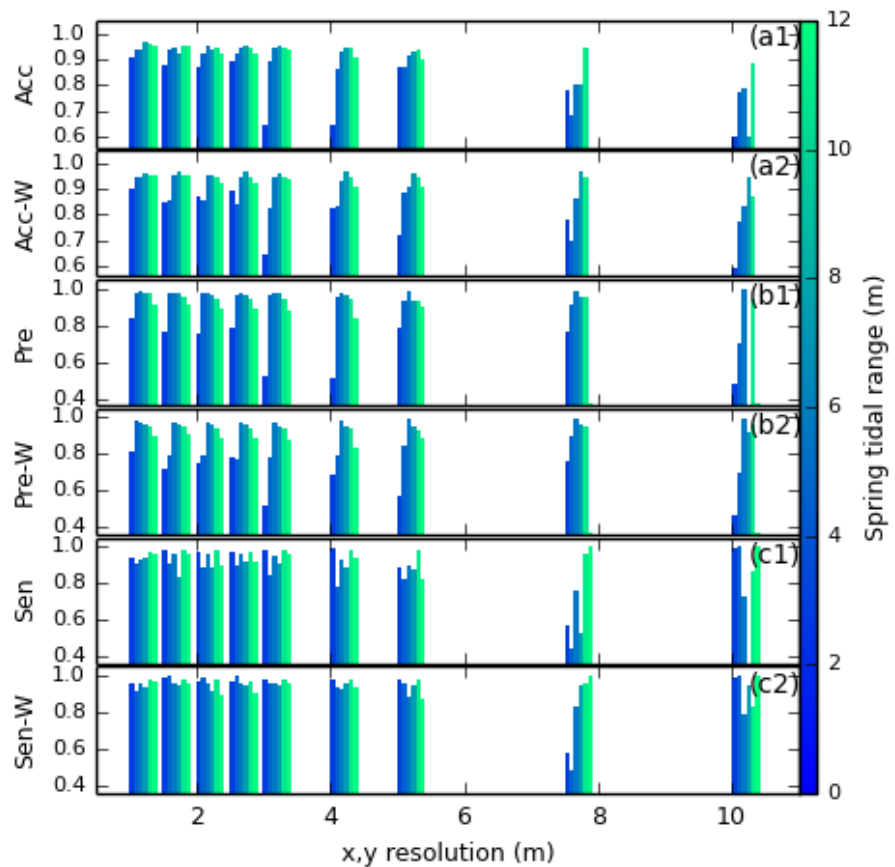


Figure 8. Performance of the platform detection method for all sites, ~~colored~~-coloured according to their spring tidal range; a1. Accuracy of the method when no filter is used; a2. Accuracy of the method when using a Wiener filter; b1. Precision of the method when no filter is used; b2. Precision of the method when using a Wiener filter; c1. Sensitivity of the method when no filter is used; c2. Sensitivity of the method when using a Wiener filter.

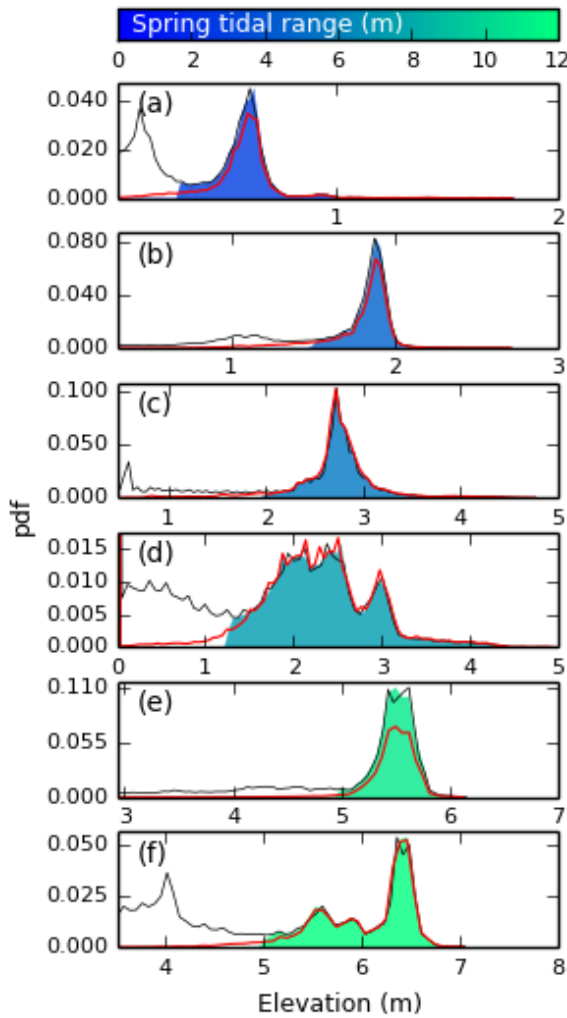


Figure 9. Total area Elevation distribution functions for sites S1 to S6 (plots a. to f. respectively) and perimeter (b) of. The red line corresponds to the marsh platform in elevation distribution for the reference rasters against. The filled area corresponds to the same data in elevation distribution of the automatically processed rasters. Data points are colored, coloured according to their spring tidal range. The grey line represents the elevation distribution of the original DEM, with transparency increasing with horizontal resolution. Points circled in red correspond frequency maxima set to match those of the automatically processed rasters in their native resolution when using a Wiener filter so as to nullify the effect of empty cells.

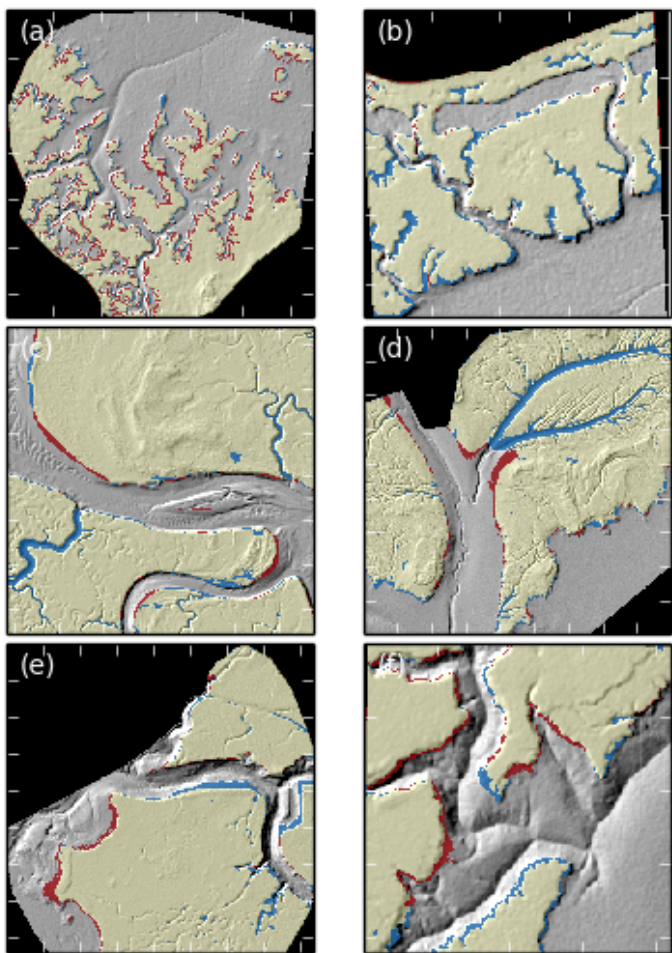


Figure 10. Rasters comparing ~~digitized~~-digitised versus extracted marsh platforms superimposed on hillshade data for all six sites after detection with no Wiener filtering. Black areas are outside of the detection domain and contain no data. Yellow areas correspond to True Positives (TP) and transparent areas to True Negatives (TN). Red areas correspond to False Positives (FP) and blue areas to False Negatives (FN). Ticks are placed 50m apart. The sites are numbered as follows: a: Shell Bay, Dorset; b: Stour Estuary, Suffolk; c: Stiffkey, Norfolk; d: Medway Estuary, Kent; e: Jenny Brown's Point, Lancashire; f: Parrett Estuary, Somerset.

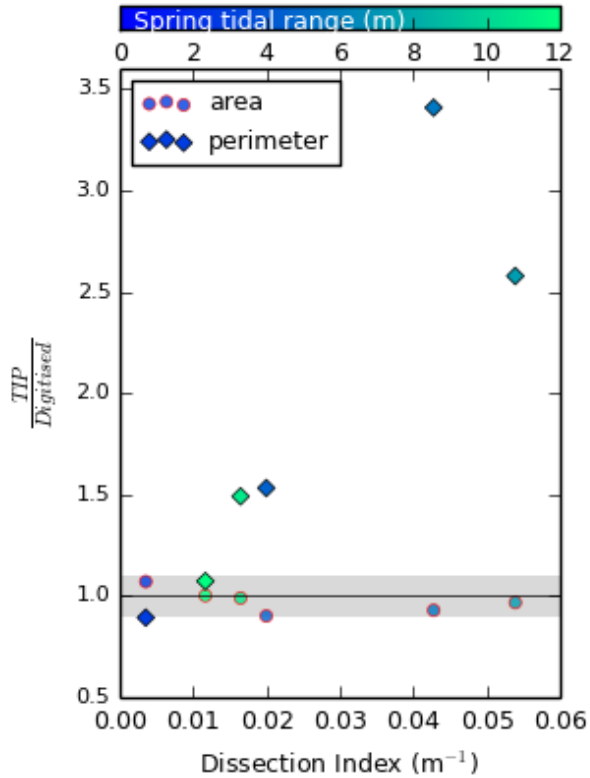


Figure 11. Elevation distribution functions. Ratio of TIP over digitised area (circles, red outlines) and perimeter (diamonds, black outlines) for sites S1 to S6 (plots a. to f. respectively). The red line corresponds to the elevation distribution for at the reference rasters native resolution of 1 m, with no Wiener filtering, as a function of dissection index. The filled area corresponds to Here, dissection index is defined as the elevation distribution ratio of the automatically processed rasters, colored according to their spring total length of tidal range. The grey line represents channels within the elevation distribution of digitised marsh platform over the original DEM, with frequency maxima set to match those area of the automatically processed rasters so as digitised marsh platform, and is not bounded by drainage basins. The greyed area corresponds to nullify a 10% buffer around the effect line of empty cells equation $y=1$.

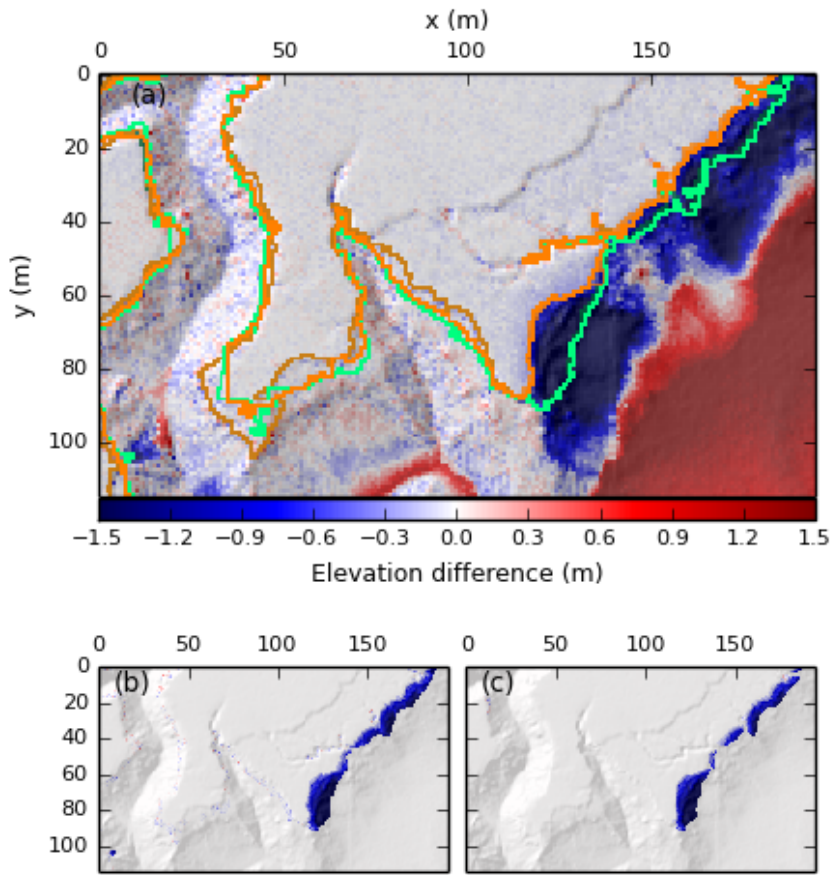


Figure 12. a. Comparison of marsh areas for a portion of S6 between March (green lines) and October (orange lines) 2007, superimposed on hillshade data of October 2007. Bright lines correspond to the automatically detected marsh boundary, whereas faded lines correspond to ~~digitized~~digitised marsh boundaries. ~~Colored~~Green faded lines are mostly covered by bright green lines. ~~Coloured~~Coloured surfaces indicate elevation gain or loss between March and October 2007; b. Map of elevation loss and gain associated to marsh platform evolution, according to the TIP method. Total volume loss is 1188 m^3 ; c. Map of elevation loss and gain associated to marsh platform evolution, according to manual ~~digitization~~digitisation. Total volume loss is 966 m^3 .

Appendix A: TIP performance tables

	S1	S2	S3	S4	S5	S6
1.0	0.907	0.94	0.936	0.967	0.963	0.952
1.5	0.876	0.934	0.948	0.926	0.953	0.95
2.0	0.868	0.921	0.95	0.942	0.945	0.919
2.5	0.891	0.926	0.948	0.955	0.942	0.926
3.0	0.646	0.897	0.944	0.954	0.946	0.935
4.0	0.643	0.861	0.932	0.942	0.945	0.909
5.0	0.869	0.872	0.915	0.927	0.941	0.897
7.5	0.778	0.682	0.804	0.806	0.942	0.376
10.0	0.599	0.771	0.786	0.603	0.882	0.376

Table A1. Table of Accuracy for sites S1 to S6 (columns) with no Wiener filter, for resolutions varying between 1 and 10 m (rows).

	S1	S2	S3	S4	S5	S6
1.0	0.837	0.979	0.985	0.972	0.973	0.916
1.5	0.763	0.97	0.977	0.974	0.952	0.91
2.0	0.753	0.971	0.976	0.967	0.941	0.89
2.5	0.789	0.961	0.976	0.969	0.942	0.889
3.0	0.518	0.959	0.975	0.974	0.943	0.88
4.0	0.513	0.951	0.977	0.968	0.942	0.835
5.0	0.787	0.936	0.989	0.932	0.932	0.896
7.5	0.765	0.908	0.988	0.956	0.949	0.376
10.0	0.475	0.699	0.992	0.0	0.947	0.376

Table A2. Table of Precision for sites S1 to S6 (columns) with no Wiener filter, for resolutions varying between 1 and 10 m (rows).

	S1	S2	S3	S4	S5	S6
1.0	0.94	0.913	0.931	0.943	0.973	0.962
1.5	0.981	0.91	0.956	0.834	0.981	0.963
2.0	0.974	0.883	0.959	0.882	0.981	0.895
2.5	0.972	0.902	0.956	0.916	0.975	0.915
3.0	0.985	0.849	0.953	0.906	0.98	0.956
4.0	0.992	0.786	0.934	0.882	0.979	0.945
5.0	0.892	0.821	0.901	0.88	0.984	0.823
7.5	0.571	0.448	0.757	0.533	0.965	1.0
10.0	0.996	1.0	0.731	nan	0.87	1.0

Table A3. Table of Sensitivity for sites S1 to S6 (columns) with no Wiener filter, for resolutions varying between 1 and 10 m (rows).

	S1	S2	S3	S4	S5	S6
1.0	0.9	0.943	0.948	0.961	0.95	0.948
1.5	0.847	0.857	0.948	0.963	0.953	0.95
2.0	0.868	0.854	0.95	0.956	0.945	0.919
2.5	0.89	0.838	0.948	0.964	0.942	0.923
3.0	0.646	0.828	0.947	0.962	0.945	0.935
4.0	0.824	0.832	0.931	0.964	0.945	0.91
5.0	0.717	0.882	0.904	0.961	0.941	0.91
7.5	0.777	0.698	0.864	0.965	0.942	0.376
10.0	0.593	0.771	0.833	0.945	0.87	0.376

Table A4. Table of Accuracy for sites S1 to S6 (columns) with a Wiener filter, for resolutions varying between 1 and 10 m (rows).

	S1	S2	S3	S4	S5	S6
1.0	0.816	0.978	0.976	0.963	0.948	0.9
1.5	0.716	0.798	0.977	0.961	0.952	0.91
2.0	0.753	0.795	0.976	0.966	0.941	0.89
2.5	0.787	0.774	0.976	0.962	0.942	0.889
3.0	0.518	0.778	0.976	0.951	0.944	0.88
4.0	0.687	0.794	0.979	0.948	0.943	0.841
5.0	0.571	0.846	0.993	0.953	0.932	0.887
7.5	0.757	0.897	0.99	0.962	0.951	0.376
10.0	0.471	0.699	0.995	0.919	0.96	0.376

Table A5. Table of Precision for sites S1 to S6 (columns) with a Wiener filter, for resolutions varying between 1 and 10 m (rows).

	S1	S2	S3	S4	S5	S6
1.0	0.955	0.92	0.957	0.938	0.982	0.971
1.5	0.993	0.997	0.956	0.945	0.981	0.963
2.0	0.974	0.993	0.959	0.92	0.982	0.895
2.5	0.973	0.999	0.956	0.946	0.975	0.909
3.0	0.985	0.961	0.955	0.953	0.977	0.956
4.0	0.976	0.936	0.931	0.961	0.979	0.938
5.0	0.978	0.958	0.883	0.948	0.985	0.873
7.5	0.581	0.489	0.834	0.95	0.964	1.0
10.0	0.996	1.0	0.79	0.946	0.838	1.0

Table A6. Table of Sensitivity for sites S1 to S6 (columns) with a Wiener filter, for resolutions varying between 1 and 10 m (rows).

Appendix B: Additional test sites and limitations of the TIP method

Here we present three additional sites that demonstrate the capabilities and limits of the TIP method. Sites were selected based on the availability of gridded 1 m DEMs on OpenTopography (<http://www.opentopography.org>) and on the variety of tidal ranges and climates present: we analyse Morro Bay, CA (A1), Wax Lake Delta, LA (A2) and Plum Island, MA (A3, see Fig.

5 B1). As is common of marshes in the United States, these additional sites have a lower relief than many European marshes, with site A2 displaying a relief of 0.8 m. The performances of the TIP method are recorded in Fig. B2. Optimisation parameters were maintained within the ranges described in Fig. 7.

Site A1, located in the North-East of Morro Bay, shows an extremely close correspondence between the digitised and TIP-detected platforms, with an accuracy of 97%. It also demonstrates the ability of the TIP method to detect marsh platforms 10 in DEMs where tidal flats exist at higher elevations, as shown by the similar and non-null probability of the TIP-detected and digitised platforms at elevations between 0.3 and 0.9 m (Fig. B2b1). To confirm the observations drawn in the body of the article, site A1 displays an abundance of false negatives within tidal creeks (Fig. B2a1), adding weight to the argument that these features require independent treatment.

Site A2 is located on the inside of a marsh island in the rapidly growing Wax Lake Delta. In order to detect the marsh 15 platform with the performance reported in Fig. B2b2, the minimum elevation buffer of 20 cm used in step 5 of Fig. 1 to fill marsh platforms was reduced to 5 cm. This allows the TIP method to function in a site with very low relief and poorly defined scarps. However, we note in Fig. B2b1 that the marginal patches of the marsh are not well identified by the method, as indicated by the relatively large number of false positives on the outline of the marsh. This example therefore demonstrates the difficulties 20 experienced when attempting to detect a prograding marsh by the TIP method. We therefore recommend caution when using the TIP method to monitor prograding marshes, as additional work is needed to fully characterise the topographic signatures of fallen blocks and pioneer zones.

Site A3 is a portion of the well-studied Plum Island, MA. The TIP method yields similar results to site A1, with the notable 25 exception of the bottom right corner of Fig. B2c1. In this area, the marsh platform is heavily dissected by wide, shallow pools and channels, which are commonly excluded from the platform ensemble by the TIP method. Furthermore, the excluded area (containing most false negatives) forms a low, shallow concave surface within the marsh, typically associated with seasonally vegetated areas. These features are morphologically similar to a high tidal flat within the platform, and are therefore difficult to identify using the TIP method.

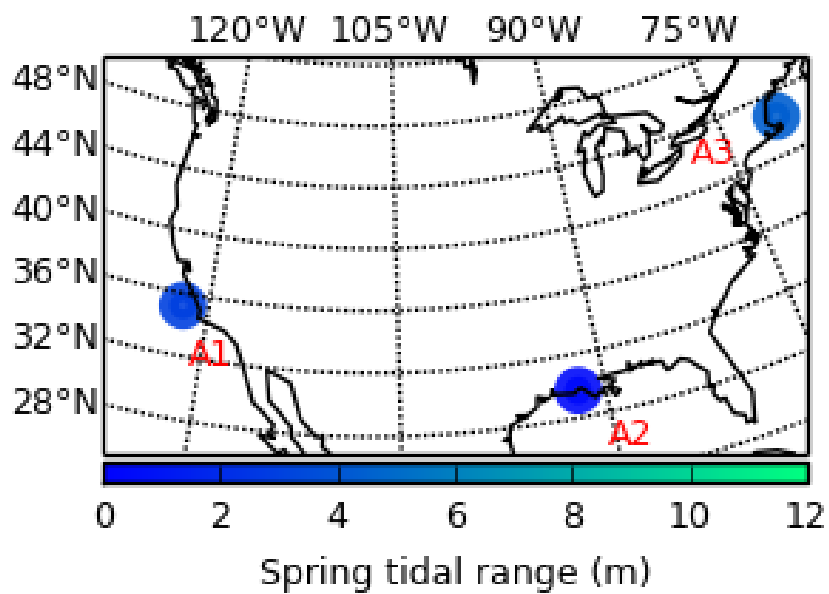


Figure B1. This map shows the three additional sites selected from the lidar collection of OpenTopography (<http://www.opentopography.org>), coloured by spring tidal range. The sites are numbered as follows: A1: Morro Bay, California; A2: Wax Lake Delta, Louisiana; A3: Plum Island, Massachusetts.

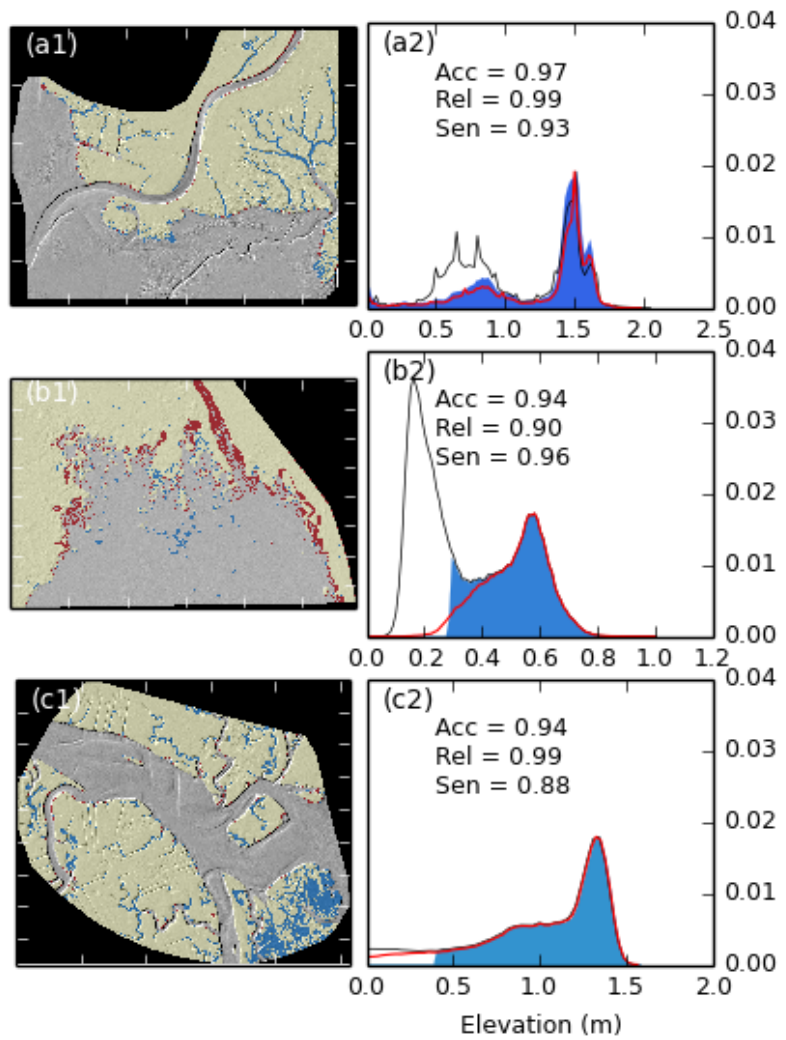


Figure B2. This figure combines the map found in Fig. 10 (a1, b1 and c1) and the probability distribution functions in Fig. 9 as well as the values of Accuracy, Precision and Sensitivity for sites A1 to A3 (a2, b2, c2). Each DEM was processed at its native resolution of 1 m.